이학박사 학위논문

일산화 탄소에 의한 혈관 내피 세포의 노화 및 급성 폐 손상에 미치는 영향

Effects of Carbon Monoxide on Endothelial Cell Senescence and Acute Lung Injury

울 산 대 학 교 대 학 원

생 명 과 학 과

진 우 빙

일산화 탄소에 의한 혈관 내피 세포의 노화 및 급성 폐 손상에 미치는 영향

지도교수 정헌택 · 박정우

이 논문을 이학박사 학위논문으로 제출함

2022 년 8 월

울 산 대 학 교 대 학 원

생 명 과 학 과

진 우 빙

진우빙의 이학박사 학위논문을 인준함

심사위원장 백승훈 인

심사위원 정헌택 인

심사위원 박정우 인

심사위원 최혜선 인

심사위원 소홍섭 인

울 산 대 학 교 대 학 원

2022 년 8 월

Effects of Carbon Monoxide on Endothelial Cell Senescence and Acute Lung Injury

This certifies that the dissertation

of YuBing Chen is approved by

Committee Chair Dr. SUNG HOON BACK

Committee Member Dr. HUN TAEG CHUNG

Committee Member Dr. JEONG WOO PARK

Committee Member Dr. HYE SEON CHOI

Committee Member Dr. HONG SEOB SO

Department of Biological Science

Ulsan, Korea

August 2022

Effects of Carbon Monoxide on Endothelial Cell Senescence and Acute Lung Injury

Supervisor: Prof. Dr. Hun Taeg Chung and Jeong Woo Park

A Dissertation

Submitted to

The Graduate School of the University of Ulsan

In the partial Fulfillment of the Requirements

for the degree of

DOCTOR OF PHILOSOPHY

BY

YUBING CHEN

Department of Biological Science

Ulsan, Korea

August 2022

Effects of Carbon Monoxide on Endothelial Cell Senescence and Acute Lung Injury

PARTⅡ

TTP activation by CO ameliorates ALI via inhibition of SARM1-dependent ferroptosis

SUMMARY

Carbon monoxide (CO) is an inert, nonreactive gas molecule, has long been known as toxic due to its capacity to bind hemoglobin and disturb oxygen transport. But low dose of CO has attracted particular attention as a potential therapeutic agent because of its reported anti-inflammation, antioxidant, anti-apoptotic and cell-protective effect. We discuss recent progress in identifying new effector systems and elucidating the mechanisms of action of CO on endothelial senescence, as well as acute lung injury (ALI). Endothelial senescence is the main risk factor that contributes to vascular dysfunction and the progression of vascular disease. Firstly, we evaluate the effects of CO on endothelial senescence and to investigate the possible mechanisms underlying this process. We measured the levels of senescence associated-β-galactosidase (SA-β-gal) activity, senescence-associated secretory phenotype (SASP), reactive oxygen species (ROS) production, and stress granule (SG) in human umbilical vein endothelial cells (HUVECs). We found that 5-fluorouracil (5FU)-induced ROS generation was inhibited by CO-releasing molecules (CORM)-A1 treatment, and endothelial senescence induced by 5FU was attenuated by CORM-A1 treatment. The SIRT1 inhibitor EX527 reversed the inhibitory effect of CO on the 5FU-induced endothelial senescence. Furthermore, SIRT1 deficiency abolished the stress granule formation by CO. Our results suggest that CO alleviates the endothelial senescence induced by 5FU through SIRT1 activation and may hence have therapeutic potential for the treatment of vascular diseases.

In addition, we further confirm the protective role of CO in ALI. we measured cell viability, lipid ROS generation and the mRNA levels of prostaglandin-endoperoxide synthase 2 (PTGS2) as well as sterile alpha and Toll/interleukin-1 receptor motif-containing 1(SARM1) in human lung epithelial cells A549 cells and mouse lung epithelial cell line MLE12 cells for in vitro

experiments. We also used *TTP*$^{+/+}$ and *TTP*$^{-/-}$ mouse lung tissue for PTGS2 and SARM1 mRNA expression measurement for in vivo experiment. We found that LPS treatment induced lipid ROS generation, upregulation of PTGS2 level as well as SARM1 expression and downregulation of the cell viability while were restored by CO-releasing molecules-2 (CORM2) treatment. Additionally, TTP activation triggered by CORM2 treatment attenuated the upregulation of SARM1 and PTGS2 induced by LPS. Furthermore, TTP deficiency abolished the PTGS2 and SARM1 downregulation induced by CO. Our results showed the mechanism that TTP activation by CO ameliorates SARM1-dependent ferroptosis. We identified SARM1, one of NAD-consuming enzymes, can be degraded by TTP resulted in inhibition of lipid ROS generation and downregulation of PTGS2, leading to ameliorate ferroptosis. Thus, the crosstalk between TTP and SARM1 provides a mechanism of control the resolution of inflammation and cell death in ALI. In conclusion, CO might contribute to cellular therapies for vascular diseases and ALI.

PART Ⅰ

CO ameliorates endothelial senescence induced by 5-fluorouracil through SIRT1 activation

Arch Biochem Biophys. 2019 Nov 30;677:108185.

I-I. ABSTRACT

Endothelial senescence is the main risk factor that contributes to vascular dysfunction and the progression of vascular disease. Carbon monoxide (CO) plays an important role in preventing vascular dysfunction and in maintaining vascular physiology or homeostasis. The application of exogenous CO has been shown to confer protection in several models of cardiovascular injury or disease, including hypertension, atherosclerosis, balloon-catheter injury, and graft rejection. However, the mechanism by which CO prevents endothelial senescence has been largely unexplored. The aim of this study was to evaluate the effects of CO on endothelial senescence and to investigate the possible mechanisms underlying this process. We measured the levels of senescence-associated-β-galactosidase (SA-β-gal) activity, senescence-associated secretory phenotype (SASP), reactive oxygen species (ROS) production, and stress granule (SG) in human umbilical vein endothelial cells (HUVECs) and the WI-38 human diploid fibroblast cell line. We found that 5-fluorouracil (5FU)-induced ROS generation was inhibited by CO-releasing molecules (CORM)-A1 treatment, and endothelial senescence induced by 5FU was attenuated by CORM-A1 treatment. The SIRT1 inhibitor EX527 reversed the inhibitory effect of CO on the 5FU-induced endothelial senescence. Furthermore, SIRT1 deficiency abolished the stress granule formation by CO. Our results suggest that CO alleviates the endothelial senescence induced by 5FU through SIRT1 activation and may hence have therapeutic potential for the treatment of vascular diseases.

I-II. INTRODUCTION

Vascular endothelial cells play a pivotal role in regulating hemostasis of the cardiovascular system, including vascular tone, balance between thrombosis and thrombolysis, recruitment of inflammatory cells to the vasculature, and platelet aggregation [1]. Oxidative stress in endothelial cells is a major stimulus for the induction of senescence. Reactive oxygen species (ROS) generated from DNA damage induces senescence in endothelial cells [2]. Endothelial senescence results in endothelial dysfunction and promotes the progression of vascular diseases such as atherosclerosis, subsequently increasing cardiovascular risk. Thus, therapies targeting endothelial senescence have important clinical implications for the treatment of cardiovascular diseases.

5-fluorouracil (5FU) is a fluoropyrimidine chemotherapeutic agent that has been widely used to treat solid cancers [3]. 5FU is also a potent antimetabolite that causes RNA miscoding and inhibits DNA synthesis via two separate mechanisms [4]. 5FU induces the senescence of endothelial cells [4] and cancer cells [5]. During 5FU-triggered senescence, endothelial nitric oxide synthase (eNOS) and SIRT1 are the most important signaling enzymes of endothelial cell homeostasis [4]. The mammalian NAD^+-dependent deacetylase SIRT1 is a crucial regulator of cell stress response and cell senescence [6,7]. SIRT1 is activated under metabolic stress conditions, and this activation orchestrates the functional changes of multiple metabolic pathways, which are important for cellular adaptation to nutrient deprivation [7]. SIRT1 is also activated by ROS [8], which endows cellular tolerance against oxidative stress-induced injuries [9]. The inhibition of SIRT1 promotes senescence, whereas increased SIRT1 function retards the development of cell senescence [7]. eNOS produces NO and exerts multiple beneficial

functions, such as vasorelaxation, anti-inflammation and anti-apoptosis, in the vasculature and thus plays a critical role in vascular homeostasis and disorders [10].

Endogenous levels of carbon monoxide (CO) result from the presence of heme oxygenase (HO)-2, which is constitutively expressed, and of HO-1 enzyme, which is an inducible enzyme responsible for the catabolism of heme products [11]. Among the HO-1 end products, CO is the most important for preventing vascular dysfunction and maintaining vascular physiology or homeostasis [12]. HO-1 expression and/or the application of exogenous CO has been shown to confer protection in several models of cardiovascular injury or disease, including hypertension and atherosclerosis [13]. However, the mechanism by which CO prevents endothelial senescence has been largely unexplored.

Stress granules (SGs) are membrane-less organelles that have a cytoprotective role and represent the sites of RNA triage during environmental assaults [14]. The formation of SGs can be initiated by the Ras GTPase-activating protein-binding protein 1 (G3BP1), T-cell intracellular antigen-1 (TIA-1), TIA-1-related (TIAR) and other proteins [15–18] and the granules are disassembled when the stress subsides [19]. A previous study found that SGs in senescent cells can decrease p21 by inhibiting its translation [20] and prevent apoptosis by minimizing energy expenditure as well as improving cell survival under damaging conditions [21]. In our previous study, SGs were found to be induced by CO [22].

Here, we found that CO attenuated 5FU-induced senescence by increasing SIRT1 expression and inducing SGs assembly in endothelial cells. Taken together, we suggest a new mechanistic explanation for the beneficial effect of CO on vascular homeostasis and disease.

I-III. MATERIALS AND METHODS

1. Materials

5FU, sodium boranocarbonate (CORM-A1), Thapsigargin (Tg), EX527 (SIRT1 inhibitor), and N-acetyl-cysteine (NAC) were purchased from Sigma Aldrich (St. Louis, MO). CO-depleted inactive form (iCORM-A1, 40μM) as a negative control was generated by dissolving CORM-A1 in 0.1M HCl and bubbling pure N2 through the solution [23].

2. Cell Culture

HUVECs were cultured on gelatin at 37°C in a humidified atmosphere of 5% CO2 and 95% air in Endothelial Cell Basal Medium 2 (EBM-2) (Lonza Clonetics, Walkersville, MD) and expanded in Endothelial Growth Medium-2 (EGM-2) singleQuots (Lonza Clonetics, Walkersville, MD). Cells used for experiments were at passages three to five. WI-38 fibroblast cells were cultured in Minimum Essential Medium (MEM, Thermo Fisher Scientific, Waltham, MA) with 10% fetal bovine serum (Gibco origin, Australia) and 1% penicillin streptomycin solution (Gibco 15140-122, Grand Island, NE) at 37°C in a humidified incubator containing 5% CO_2.

3. SA-β-gal staining

Senescence-associated (SA)-β-Galactosidase (gal) characterizes senescence because the lysosomal content increases and has residual activity at suboptimal pH 6 [24]. To observe the senescent cells, WI-38 cells and HUVECs were treated with 5FU to induce premature cellular senescence. Then, SA-β-gal staining was performed by utilizing a cellular senescence cell

histochemical stain kit (Sigma CS0030, Saint Louis, MO) according to the manufacturer's protocol.

4. Cell viability assays

(The WST-8 QuantiMax™-Cell viability assay kit) was used to analyze cell viability according to the manufacturer's instructions. HUVECs (1×10^4/well) were plated onto 96-well plates. All assays were performed in triplicate. Cells in each well were suspended in 100μL fresh medium containing the various treatment and then seeded. After treatment, WST-8 (10 μL/well) was added for 4h of additional incubation, and the absorbance was measured at 450nm.

5. Intracellular ROS measurement

HUVEC cells were pretreated with CORM-A1 (40mM) for 1h followed by the stimulation of 5FU (70μg/ml) for 48h. Cells were post-treated with CORM-A1 (40μM) every 24h. For positive control, HUVEC cells were co-treated with NAC (3 mM) and 5FU (70μg/ml) for 4h, and then cells were supplied with fresh medium. Then, the cells were trypsinized, placed in fluorescence-activated cell sorting tubes, and washed with 1xPBS. Cells were incubated in 1xPBS containing 3μM CM-H_2DCF-DA (Invitrogen C6827, Eugene, OR) for 40min at 37°C. DCF-DA fluorescence was detected by using a flow cytometry (FACSCanto II), and data was analyzed by FlowJo V10 software (Tree Star Inc., San Carlos, CA). The fold of change is presented by geometric mean fluorescence intensity. To evaluate the intracellular ROS production by confocal microscopy, HUVEC cells were grown in confocal 4-well chambers (#155382, Nunc, Thermo Scientific, Waltham, MA). The production of intracellular ROS was

detected by staining with CM-H_2DCFDA (10μM) for 15min in 1xPBS. Images were observed by using Olympus FV1200 confocal microscope (Olympus, Tokyo, Japan).

6. RNA isolation and real-time quantitative PCR (RT-qPCR)

After indicated treatment, HUVECs and WI-38 cells were lysed using TRIzol reagent (Invitrogen, Carlsbad, CA), and total RNA was isolated. We used 2μg total RNA to synthesize cDNA using M-MLV reverse transcriptase (Promega, Madison, WI). The synthesized cDNA was subject to PCR-based amplification. The samples were free of genomic DNA. To perform quantitative real-time PCR (qRT-PCR), the synthesized cDNA was amplified with SYBR Green qPCR Master Mix (2x, USB Production; Affymtrix) on ABI 7500 Fast Real-time PCR system (Applied Biosystems, Carlsbad, CA). The following qRT-PCR primers were used: human GAPDH (forward: 5′-CAA TGA CCC CTT CAT TGA CCT C-3′, reverse: 5′-AGC ATC GCC CCA CTT GAT T-3′), human p21 (forward: 5′-CGA TGG AAC TTC GAC TTT GTC A 3′, reverse: 5′-GCA CAA GGG TAC AAG ACA GTG-3′), human PAI-1 (forward: 5′-TGA TGGCTC AGA CCA ACA AG-3′, reverse: 5′-CAG CAA TGA ACA TGC TGA GG-3′), human TNF-α (forward: 5′-GCT GCA CTT TGG AGT GAT CG-3′, reverse: 5′-GTT TGC TAC AAC ATG G GC TAC AG-3′), and human HO-1 (forward: 5′-CAG GAG CTG CTG ACC CAT GA 3′, reverse: 5′-AGC AACTGT CGC CAC CAG AA-3′).

7. Western blot

Total proteins extracted from harvested cells were prepared in Mammalian Cell-PE L™ Buffer (Organic buffer + 10 mM NaCl + Detergent, pH7.5) (GBiosciences, USA) containing

phosphatase (SIGMA-Aldrich, St. Louis, MO), and protease inhibitors (SIGMA-Aldrich, St. Louis, MO). Protein concentration was determined using the BCA protein assay kit (Pierce Biotechnology, Rockford, IL). For western blots, protein samples were separated using SDS-PAGE and transferred onto polyvinylidene difluoride me branes (Millipore, Burlington, MA).The membrane was blocked with 5% skim milk (BD Difco™ Skim Milk, PA) in phosphate buffered saline Tween 20 (PBS-T) and then incubated with a primary antibody against eNOS (1:1000 v/v in PBS-T, BD Bioscience, San Jose, CA), SIRT1 (1:1000 v/v in PBS-T, millipore, Burlington, MA), β-actin (1:2000 v/v in PBS-T, Invitrogen, Carlsbad, CA) followed by incubation with a secondary antibody.

8. Immunofluorescence

To observe the formation of SGs, HUVECs were plated on 4-well Lab-Tek chambered cover-glass (Nunc, Thermo Scientific, Waltham, MA), and pretreated with iCORM-A1 (40 μM) or CORM-A1 (40 μM), followed by the administration of 5FU and thapsigargin (Tg, 200nM) as a positive control to induce premature cellular senescence. After treatment, the cells were fixed with 10% neutral-buffered formalin solution (Sigma Aldich, St. Louis, MO) for 15min. The cells were subsequently permeabilized with 0.1% Triton X-100. The cells were then incubated in blocking solution (3% BSA) for 1h at room temperature to reduce nonspecific binding of the antibody. Incubation with the primary antibodies was carried out for overnight at 4°C. The following primary antibodies were used: anti-TIA-1 (1:500, Abcam, Cambridge, MA) and anti-G3BP1 (1:500, Santa Cruz Biotechnology, CA, USA). Alexa-Fluor 488 anti-mouse (1:500, Invitrogen, Carlsbad, CA) and Alexa-Fluor 594 anti-rabbit (1:500, Invitrogen, Carlsbad, CA) IgG antibodies were used as secondary antibodies. Then, the cells were washed with PBS-T

followed by DAPI (Sigma, St. Louis, MO) staining. Images of the cells were obtained using an Olympus FV1200 confocal microscope (Olympus, Tokyo, Japan).

9. Statistics

For statistical comparison, all data were presented as mean ± SD (n =3). The comparison among all experimental groups were made by One-way ANOVA with Tukey's post hoc tests, and all statistical analysis were assessed by GraphPad Prism software version 5.03 (SanDiego, CA). The changes among groups with probability values of $p \leq 0.05$ were considered statically significant.

I-IV. RESULTS

Senescence of HUVECs in response to increasing concentrations of 5FU

Previous study already identified that 5FU induces senescence of EA. hy926 human endothelial cells, so we firstly confirm this effect of 5FU in human umbilical vein endothelial cells (HUVECs), To elicit the endothelial senescence, HUVECs were incubated for 4h with different concentrations of 5FU (Fig. 1A). After this treatment, senescence was assessed as a percentage of SA-β-gal. 5FU significantly enhanced the proportion of SA-β-gal-positive cells (Figs. 1A and B) and induced the mRNA expression of p21 in a dose-dependent manner (Fig. 1C). Thus, 70μg/ml of 5FU was chosen because it was the most pro-senescent and no apoptosis was found in the preliminary assessment (Fig. 1D). Altogether, these data confirm that 5FU had the most profound effect on HUVECs senescence.

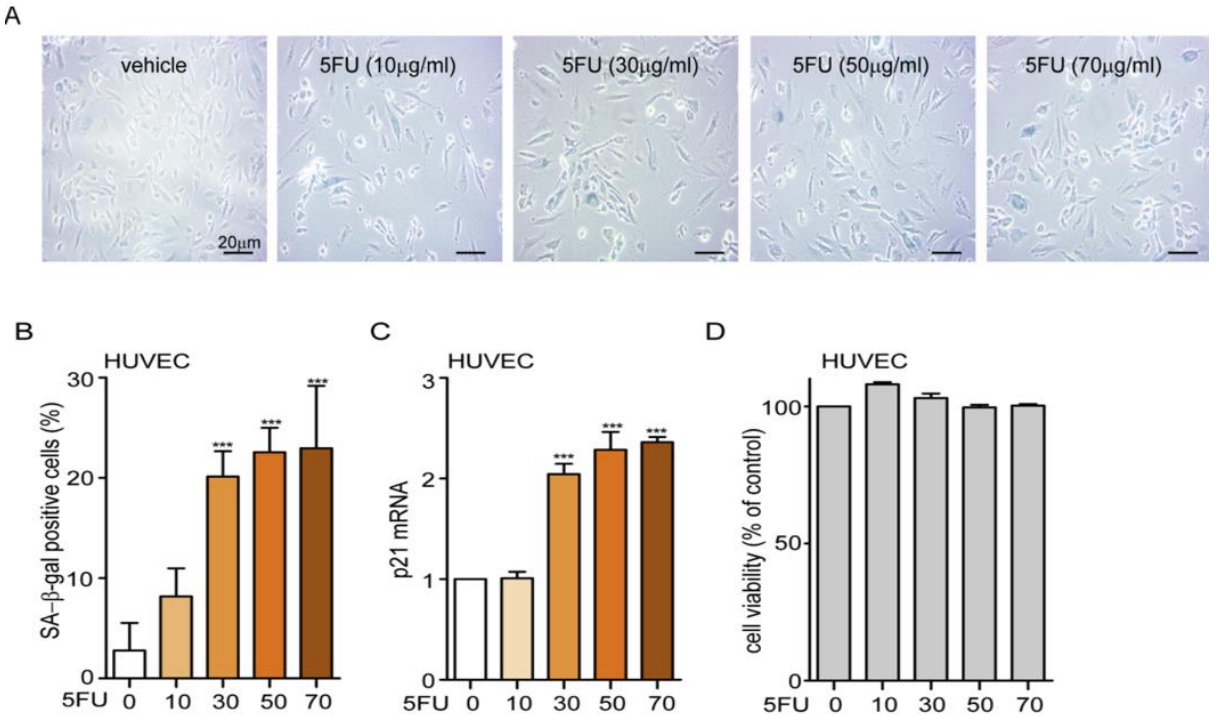

Fig. 1. Senescence of HUVECs in response to increasing concentrations of 5FU

(A-B) HUVECs were stained for SA-β-galactosidase and treated with vehicle and 5FU (10, 30, 50, and 70 μg/ml). Representative pictures and percentage of SA-β-galactosidase positive HUVECs treated with vehicle and 5FU (10, 30, 50, and 70 μg/ml) as indicated. (C) mRNA expression of p21 detected by RT-qPCR regarding HUVECs treated with vehicle and 5FU (10, 30, 50, and 70 μg/ml) as indicated. (D) HUVECs viability after treatment 5FU was evaluated by Quanti-max™ WST-8 cell viability assay kit. Data represented are the means ± SEM of three independent experiments. $*p < 0.05$, $**p < 0.01$, and $***p < 0.001$.

CO inhibits the endothelial cell senescence induced by 5FU.

Given the established role of HO-1 in endothelial cell senescence [1], we hypothesized that CO protects against endothelial senescence induced by 5FU. To investigate the roles of CO in 5FU-induced senescence, we exposed HUVECs propagated in serum-free DMEM alone to 70 µg/ml 5FU for 4h after pre-treatment of cells for 1h with CORM-A1, a CO- releasing molecule that has been shown to deliver CO to cells [23]. CO protection was evaluated by pre-incubating for 1h with CORM A1 at 20 and 40µM. The pretreatment with CORM-A1 significantly alleviated the 5FU elicited senescence of HUVECs (Fig. 2). 5FU significantly enhanced the proportion of SA-β-gal-positive HUVECs suggesting that endothelial senescence was successfully induced by 5FU. The CO treatment alone did not alter the basal senescence level of HUVECs, but reversed 5FU-induced endothelial senescence in a dose-dependent manner (Fig. 2A and B). Therefore, these data indicated that CO inhibits the endothelial cell senescence induced by 5FU.

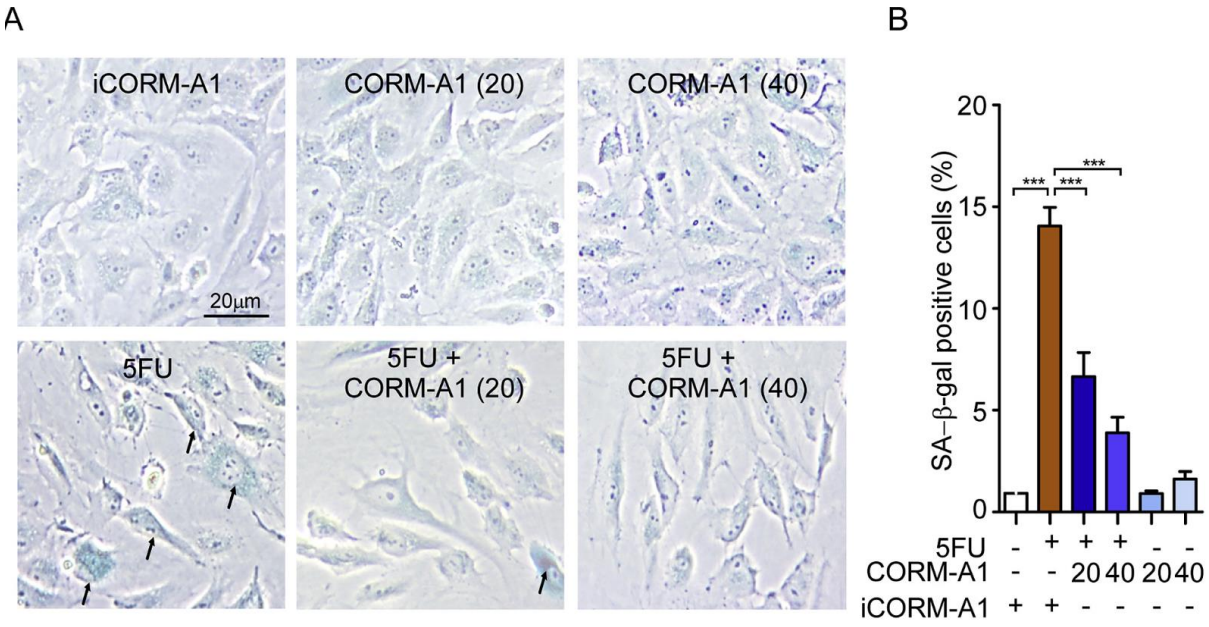

Fig. 2. CO inhibits the endothelial cell senescence induced by 5FU.

(A–B) Representative pictures and percentages of SA-β-galactosidase positive HUVECs treated with vehicle, 5FU (70 μg/ml), and CORM-A1 (20 and 40 μM) as indicated. Data represented are the means ± SEM of three independent experiments. *$p < 0.05$, **$p < 0.01$, and ***$p < 0.001$.

CO ameliorates SASP components in endothelial cell induced by 5FU.

The cyclin-dependent kinase inhibitors p21, which leads to the inhibition of the cyclin E-CDK2 complex, is regarded as an important molecule underlying endothelial senescence [2]. As shown Fig.3A, 5FU significantly upregulated the mRNA expression of p21 in HUVECs. Furthermore, CO treatment alone did not alter the basal levels of p21 expression but abolished 5FU-induced upregulation of p21 in a dose-dependent manner (Fig.3A). In previous studies, senescence was shown to confer characteristic changes in gene expression, such as inflammatory adhesion molecules, cytokines, and matrix metalloproteinases, collectively referred to as the senescence associated secretory phenotype (SASP) [25-27]. The SASP defines the ability of senescent cells to express and secrete a variety of extracellular modulators [28–30]. To determine whether treatment with CORM-A1 induced manifestation of SASP components, we assessed the prothrombotic plasminogen activator inhibitor-1 (PAI-1), as well as cytokine TNF-α, shown previously to be elevated in endothelial cells at replicative senescence [31–34]. 5FU significantly increased PAI-1 and TNF-α expression, and the upregulation of these SASPs was attenuated by CO treatment (Fig.3B and C). Additionally, CORM-A1 inhibited the PAI-1 secretion increased by 5FU (Fig.3D). Hence, these data demonstrated that CO inhibits the senescence induced by 5FU in HUVECs.

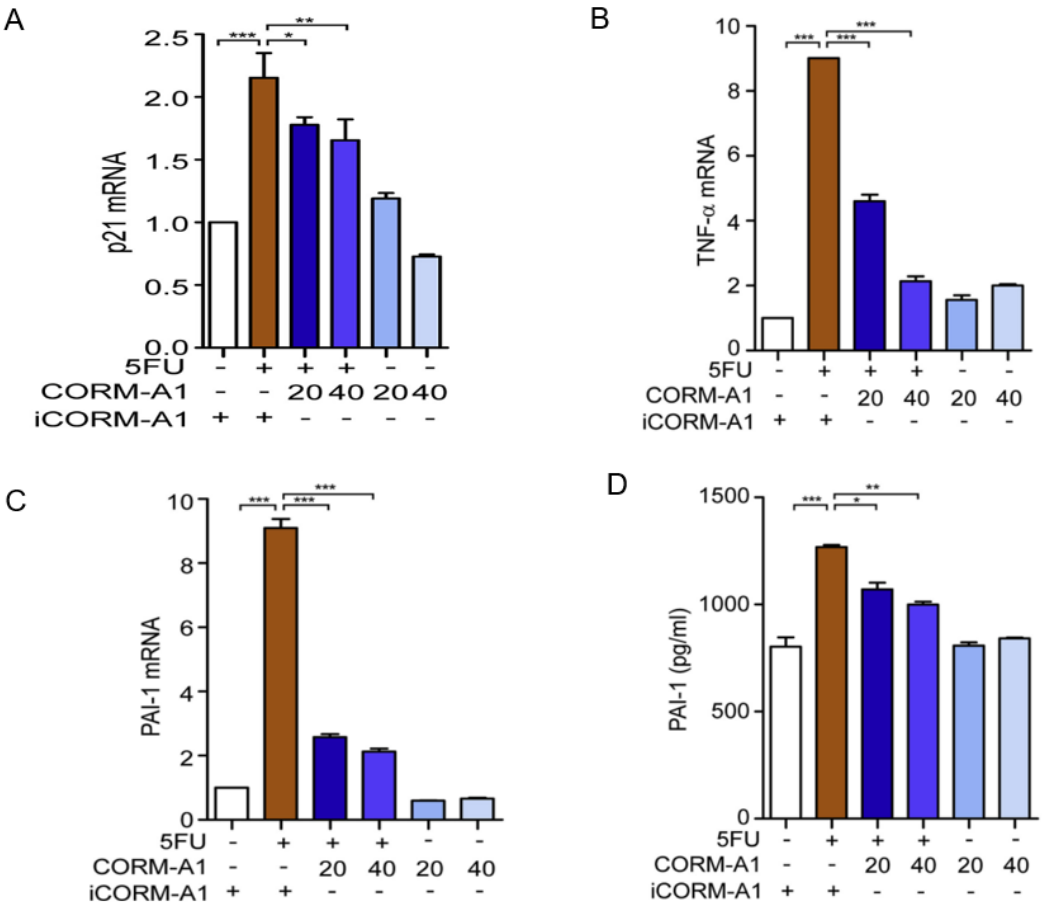

Fig. 3. CO ameliorates SASP components in endothelial cell induced by 5FU.

(A-B) The mRNA expression of p21 (A) and SASP (TNF-α) (B) were detected by RT-qPCR after HUVECs were treated with vehicle, 5FU (70 μg/ml) and CORM-A1 (20 and 40 μM) as indicated. (C) mRNA expression of PAI-1 was detected by RT-qPCR after HUVECs were treated with vehicle, 5FU (70 μg/ml) and CORM-A1 (40 μM) as indicated. The concentration of PAI-1(D) in cultured media was detected by ELISA. Scale bars are equal to 20 μm. Data represented are the means ± SEM of three independent experiments. *$p < 0.05$, **$p < 0.01$, and ***$p < 0.001$.

CO inhibits SASP components in human lung fibroblast induced by 5FU.

In addition to endothelial cells, human fibroblasts (WI38 cells) were used to study cellular senescence, as WI38 cells divide a limited number of times and cease growing. This phenomenon is known as cellular replicative senescence [25]. As shown Fig. 4A, 5FU significantly upregulated the mRNA expression of p21 in WI38 cells. Furthermore, CO treatment alone did not alter the basal levels of p21 expression but abolished 5FU-induced upregulation of p21. (Fig.4A) 5FU significantly increased TNF-α and PAI-1 expression in WI38 cells, and the upregulation of these SASPs was attenuated by CO treatment (Fig.4B and C). Furthermore, CORM-A1 inhibited the PAI 1 secretion increased by 5FU (Fig.4D). Altogether, these data demonstrated that CO also can inhibit the senescence induced by 5FU in WI38 cells.

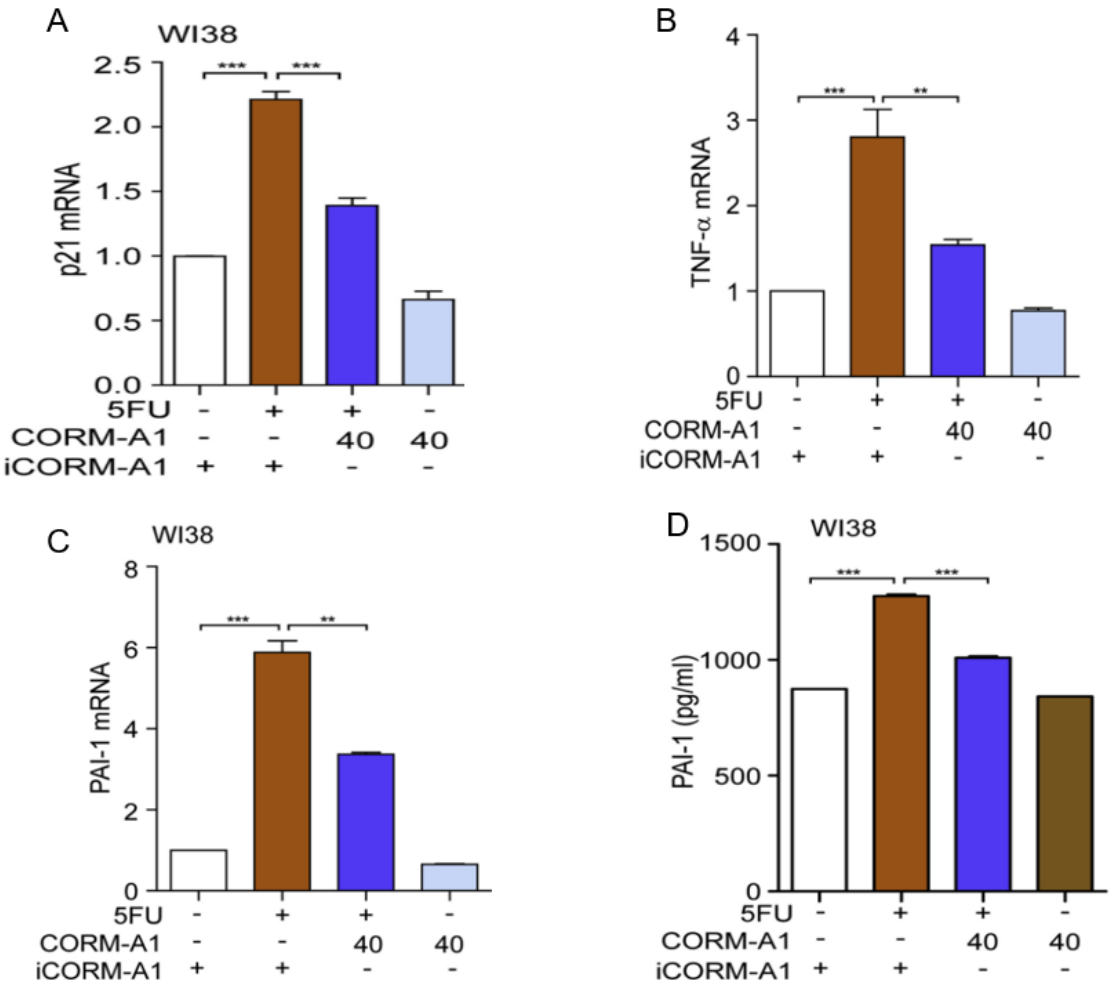

Fig. 4. CO inhibits SASP components in human lung fibroblast induced by 5FU.

(A-C) The mRNA levels of p21 (A) TNF-α (B), and PAI-1 (C) were detected by RT-qPCR after treatment with iCORM-A1 (20 and 40 μM), 5FU (70 μg/ml), and CORM-A1 (20 and 40 μM) as indicated. (D) The levels of PAI-1 protein were measured in WI38 cells treated with iCORM-A1 (20 and 40 μM), 5FU (70 μg/ml) and CORM-A1 (20 and 40 μM). Data represented are the means ± SEM of three independent experiments. *$p < 0.05$, **$p < 0.01$, and ***$p < 0.001$.

CO reduced ROS generation induced by 5FU

Specific increases of ROS levels have been demonstrated as being critical for the induction and maintenance of the cell senescence process [35]. According to a previous study, CO may be required to suppress ROS generation [36]. To evaluate whether CO has an antioxidant effect, we measured the production of intracellular ROS by staining with CM-H_2DCF-DA. As shown in Fig. 5A, CORM-A1 treatment decreased the 5FU increased ROS production in HUVECs by analyzing with FACS. The inhibitory effect of CORM-A1 on ROS production by 5FU showed a similar result as was seen in the N-acetyl-L-cysteine (NAC)-treated group; NAC is a scavenger of ROS and was used in the positive control (Fig. 5A). CORM-A1 was confirmed to reduce the 5FU-induced ROS production by confocal microscopy (Fig. 5B). Previous studies have demonstrated that ROS reduction is dependent on HO-1 expression [28]. Thus, we assessed whether the generation of HO-1, an antioxidant molecule, by CO was involved in attenuating the cellular senescence. Most significantly, CORM-A1 treatment increased the HO-1 levels inhibited by 5FU (Fig. 5C). Therefore, CO has an antioxidant effect and reduces the ROS levels induced by CO.

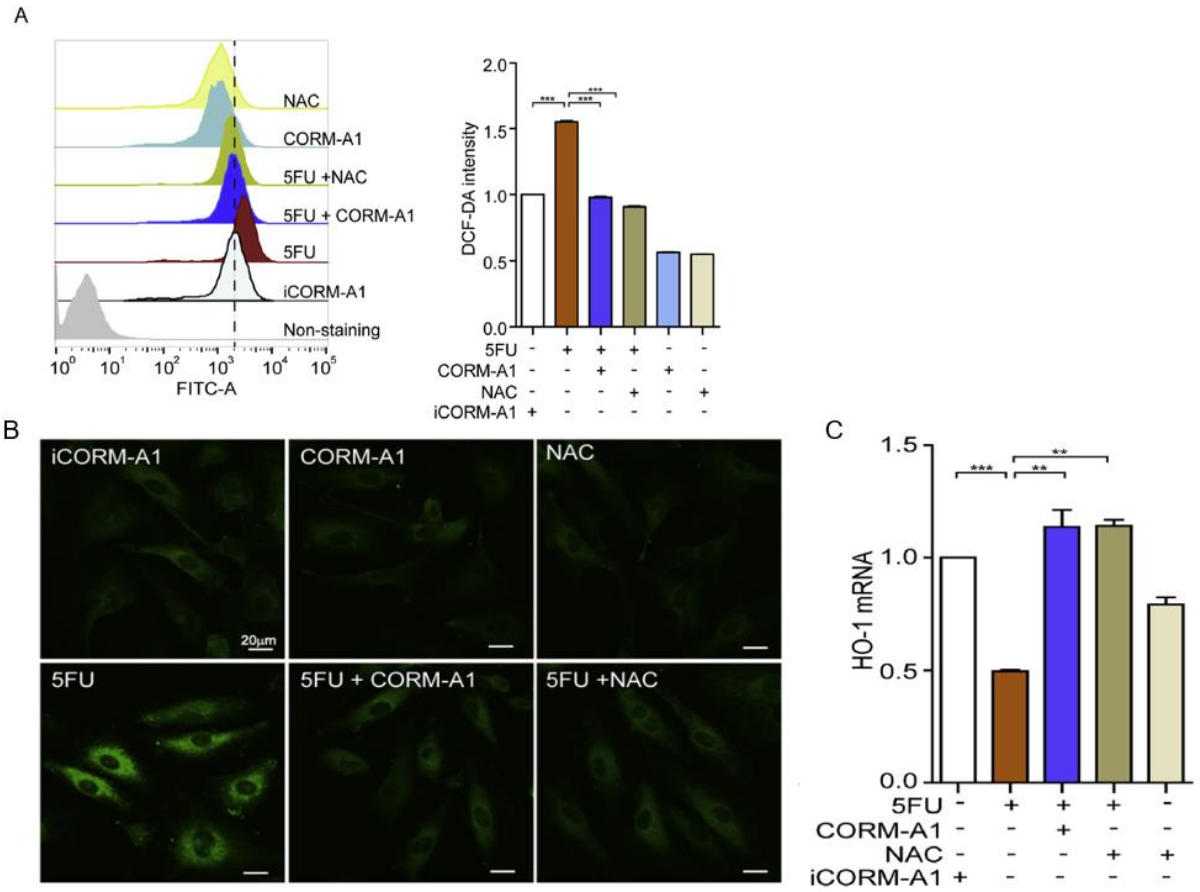

Fig. 5. Co reduced ROS generation induced by 5FU

(A)HUVEC cells were pretreated with CORM-A1 (40 μM) for 1h followed by the administration of 5FU (70 μg/ml) for 4h, and then cells were changed into fresh medium. CORM-A1 (40 μM) was post-treated for 1h each day. After a 48h incubation, the production of intracellular ROS was detected by staining with DCF-DA and examining with flow cytometry (FACSCanto II). For the positive control, HUVEC cells were co-treated with NAC (3 mM) and 5FU (70 μg/ml) for 4 h, and then cells were changed into fresh medium. The fold change of geometric fluorescence mean intensity is presented as mean ± SD (n = 3). (B) HUVEC cells were pretreated with iCORM-A1 (40 μM), CORM-A1 (40 μM), and NAC (3 mM) for 1h followed by the administration of 5FU (70 μg/ml) for 4 h, and then

cells were changed into fresh medium. After a 48h incubation, the production of intracellular ROS was detected by staining with DCF-DA and examined by confocal microscopy. (C) The scale bar represents 20μm. The mRNA expression of HO-1 in HUVEC cells were measured by RT-PCR assay. Data are expressed as means ± SD (n = 3). One-way ANOVA with Tukey's post hoc tests was per- formed; **$p < 0.01$ and ***$p < 0.001$.

CO prevents 5FU-induced cellular senescence via the reduction of intracellular ROS.

As we mentioned before, the cyclin-dependent kinase inhibitors p21 and SASP component PAI-1 are important to endothelial senescence(Fig. 3).So to investigate the effects of ROS induced by 5FU on endothelial cells, we also examined senescence-related genes p21 and PAI-1.As shown in Fig.6A and B, the levels of p21 and PAI-1 due to 5FU were shown to be higher than that of the control group while Cells pretreated with CORM-A1 exhibited markedly decreased SASP in response to 5FU. Hence, these data suggested that CO prevents 5FU-induced cellular senescence via the reduction of intracellular ROS.

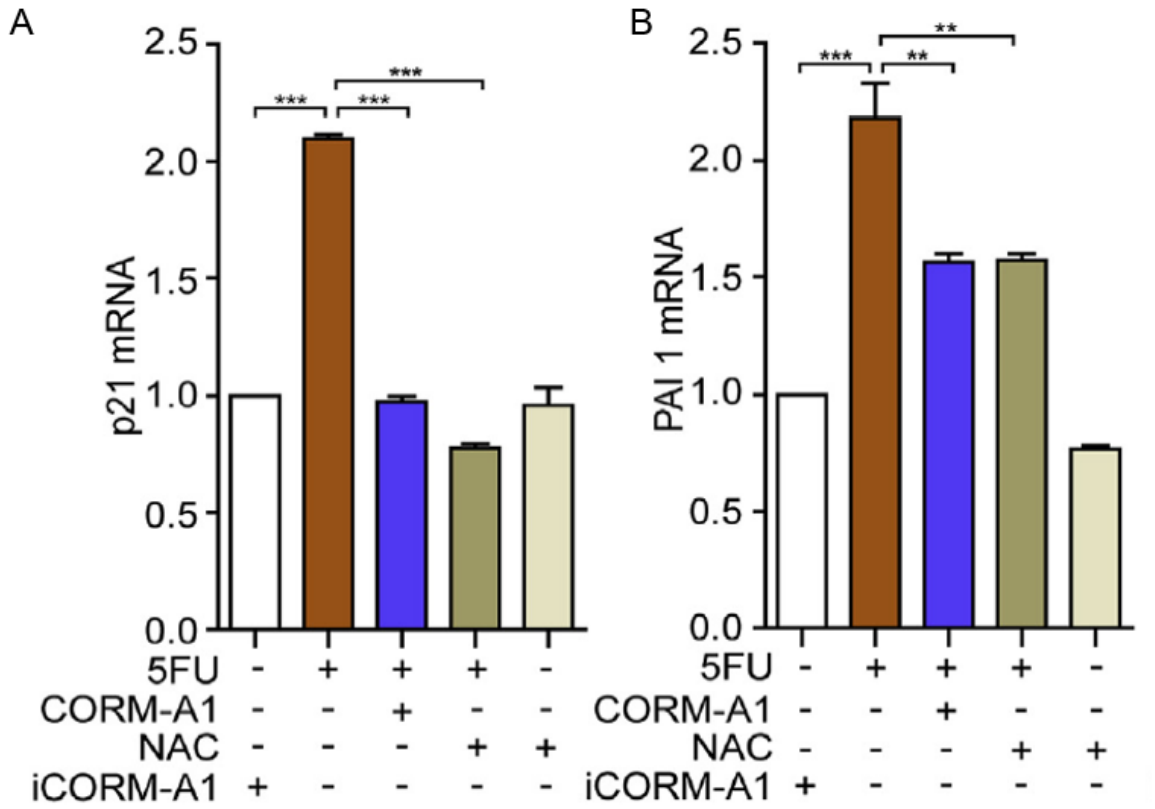

Fig. 6. CO prevents 5FU-induced cellular senescence via the reduction of intracellular ROS.

The mRNA expression of p21 (A), PAI-1 (B) in HUVEC cells were measured by RT-PCR assay. Data are expressed as means ± SD (n = 3). One-way ANOVA with Tukey's post hoc tests was performed; **p < 0.01 and ***p < 0.001.

CO reduces SASP components dependent on HO-1 in WI-38 cells.

Based on these studies, we then investigated whether CO regulates the expression of SASP that is dependent on HO-1in WI-38 cells. As shown in Fig.7A, WI-38 cells transfected with siRNA against Hmox-1 (*siHmox-1*) exhibited significantly decreased HO-1 expression compared with cells transfected with scramble RNA (*scRNA*). The HO-1 deficiency prevented the attenuation of 5FU-increased p21 or PAI-1 expression by CO (Figs.7B and 7C). To further confirm whether the influences of CO on SASP phenotype are dependent on HO-1, ZnPP was used as an inhibitor of HO-1. The increase in p21 and PAI-1 with 5FU was not suppressed by CO in the presence of ZnPP (Figs.7D and 7E). Therefore, CO also reduced SASP components dependent on HO-1 in WI-38 cells.

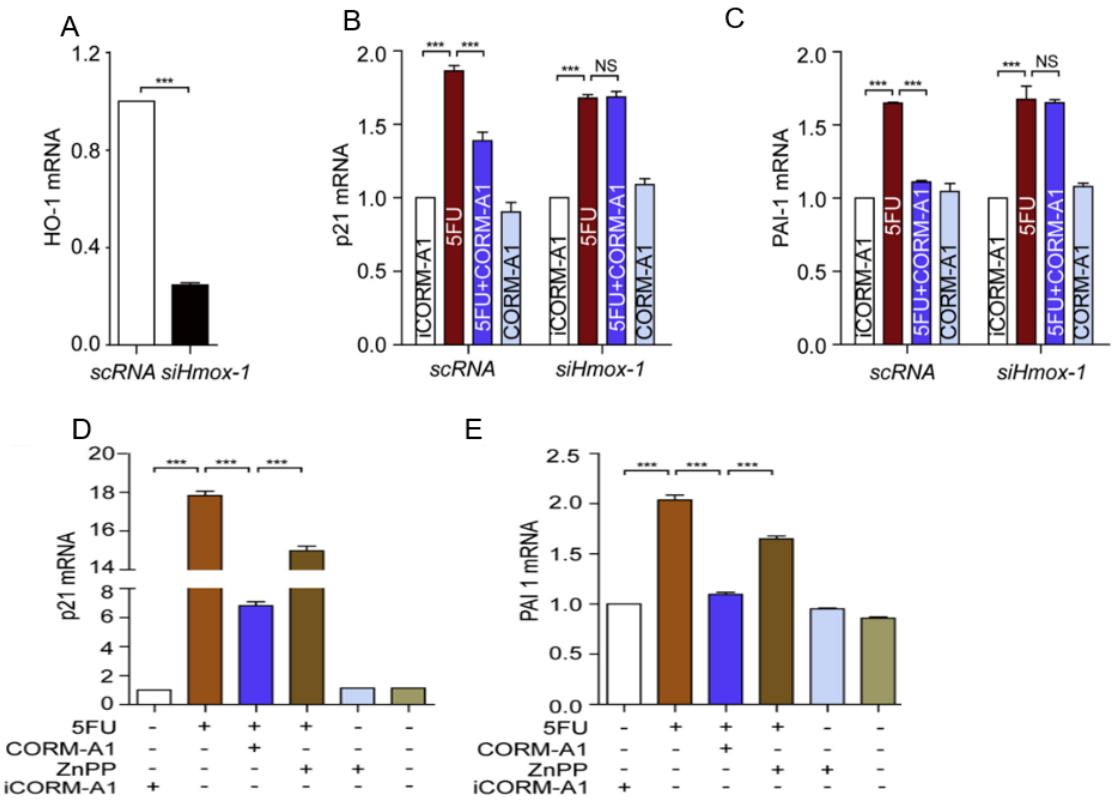

Fig.7. CO reduces SASP components dependent on HO-1 in WI-38 cells.

(A-C) WI-38 cells were transfected with scramble RNA (*scRNA*) and siRNA against *Hmox-1* (*siHmox-1*) for 36h. Then cells were treated with CORM-A1 (40 μM) for 1h followed by the stimulation of 5FU (70 μg/ml). After a 4h-treatment with 5FU, cells were supplied with fresh media, and incubated for another 72h. The mRNA levels of HO-1 (A), p21 (B) and PAI-1 (C) were detected by RT-qPCR. (D-E) WI-38 cells were pretreated with ZnPP (5 μM) for 30 min followed by the administration of iCORM-A1 (40 μM) or CORM-A1 (40 μM) for 1h. Then, cells were challenged with 5FU (70 μg/ml) for 4 h and supplied with fresh medium. After 48h incubation, the mRNA levels of p21 (D) and PAI-1 (E) were assessed by RT-qPCR. Data were expressed as mean ± SD (n = 3 per group). ***$p < 0.001$, NS: not significant.

CO reverses the downregulation of eNOS and SIRT1 expression.

We then speculated on the mechanism by which CO inhibits 5FU-induced endothelial senescence. In our previous study, we found that CO treatment increased SIRT1 expression [29]. SIRT1 is known to inhibit cellular senescence by stresses, including DNA damage and oxidative stress [30,37,38]. In addition, The NO generated by eNOS can protect cells from oxidative stress and delay endothelial cellular senescence [52,53]. To investigate the roles of CO in eNOS and SIRT1 levels, HUVECs were treated with 70μg/ml 5FU for 4h in the presence of CORM-A1. 5FU significantly decreased eNOS and SIRT1 protein expression, whereas the downregulation of eNOS and SIRT1 protein expression was increased by the CORM-A1 treatment (Fig. 8A–C). Hence, these data suggested that CO reverses the downregulation of eNOS and SIRT1 expression.

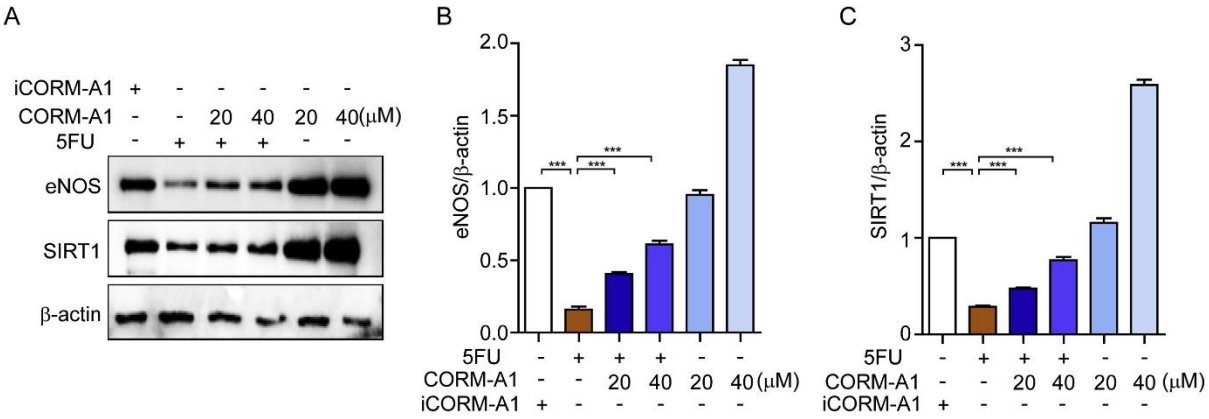

Fig. 8. CO attenuates the downregulation of eNOS and SIRT1 expression.

(A–C) HUVECs with CORM-A1 pretreatment at 20 and 40 μM for 1h were incubated with 70 μg/ml 5FU for 4h (A). The expression of eNOS (B) and SIRT1 (C) protein were evaluated by western blot analysis. The optical density of the eNOS and SIRT1 bands was normalized for

that of β-actin. Data represented are the means ± SEM of three independent experiments; *** $p < 0.001$.

CO decreases 5FU-induced endothelial senescence through SIRT1

To further confirm the role of SIRT1 in CO prevent from 5FU-induced endothelial senescence, the potent and selective SIRT1 inhibitor, EX527, was used to treat HUVECs. CORM-A1 treatment protected against 5FU-induced endothelial senescence, however, this was reversed in the EX527 treatment, as analyzed by SA-β-gal staining (Fig. 9A). The CORM-A1 treatment decreased the mRNA level of p21 in the 5FU-treated HUVECs, but not in the EX527 treated HUVECs (Fig. 9B). Additionally, the CORM-A1 treatment alleviated SASP production (PAI-1 and TNF-α) in 5FU-induced HUVECs, but not in EX527 treated HUVECs (Fig. 9C and D). SIRT1 plays an important role in the regulation of oxidative stress, therefore, we tested whether SIRT1 was related to the antioxidant function of CORM-A1 in 5FU-induced senescence. The CORM-A1 treatment increased the mRNA level of the HO-1 in the 5FU-treated HUVECs. In EX527-treated HUVECs, the CORM-A1 treatment failed to recover the HO-1 mRNA expression level (Fig. 9E). To further confirm the SIRT1 effect, we used scRNA and siRNA against SIRT1 (*siSirt1*) to transfect the HUVECs, the results showed that SIRT1 mRNA expression was significantly lower in the siSirt1 group compared to in the control group (Fig. 9F). The SIRT1 deficiency prevented CORM-A1 inhibition of 5FU-induced p21, PAI-1, TNF-α expression (Fig. 9G–I). In the presence of SIRT1, CORM-A1 recovered HO-1 expression (Fig. 9J). Thus, we could conclude that SIRT1 is required for the inhibitory effect of CO on endothelial senescence via reduction of ROS levels.

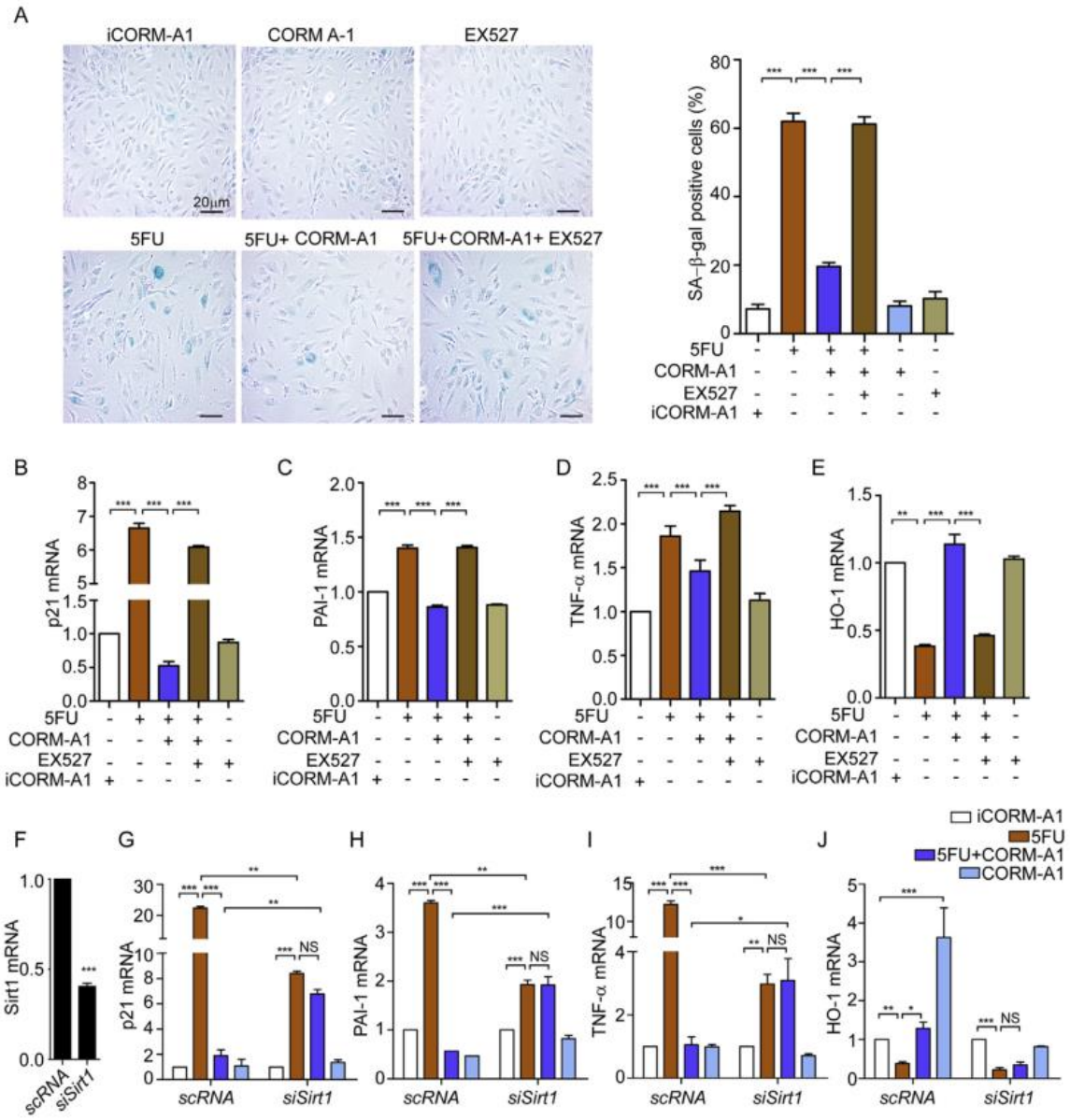

Fig. 9. CO decreases 5FU-induced endothelial senescence through SIRT1.

HUVECs were pretreated with iCORM-A1 (40 μM), CORM-A1 (40 μM), and EX527 (10 μM) for 1h followed by the stimulation of 5FU (70μg/ml) for 4h in serum-free DMEM. HUVECs were post-treated with CORM-A1 (40μM) every 24h for 2 days. (A, left panel) HUVECs were subjected to staining for SA-β-gal activity. (A, right panel) Graph represents the percentage of

cells that stained positive for SA-β-gal activity mRNA levels of p21 (B), PAI-1 (C), TNF-α (D), and HO-1 (E) were determined by RT-qPCR. (F–J) HUVECs were transfected with negative control scrambled RNA (*scRNA*) or siRNA targeted at SIRT1 (*siSIRT1*). After 36h transfection, cells were pretreated with CORM-A1 (40μM) for 1h followed by stimulation by 5FU (70μg/ ml) for 4h in serum free DMEM. Then, mRNA levels of Sirt1 (F), p21 (G), PAI-1 (H), TNF-a (I), and HO-1 (J) were determined by RT-qPCR. One-way ANOVA with Tukey's post-hoc test was performed; *$p < 0.05$, **$p < 0.01$, ***$p < 0.001$, and NS: not significant.

SIRT1 is critical for the antioxidant effect of CO in WI-38 cells

We already found CO decreases 5FU-induced endothelial senescence through SIRT1 in HUVECs, next we wondered whether the CO-triggered reduction of ROS is mediated by SIRT1 also happened in WI-38 cells, EX527 or siSirt1 transfection was used to inhibit SIRT1 activity. 5FU-increased ROS levels were decreased by CORM-A1, but not in the presence of EX527 (Fig.10A). Consistent with EX527 treatment, with SIRT1 deficiency, CORM-A1 did not decrease 5FU-increased ROS levels (Fig.10B). Thus, we could conclude that SIRT1 is required for the inhibitory effect of CO on endothelial senescence via reduction of ROS levels in WI-38 cells.

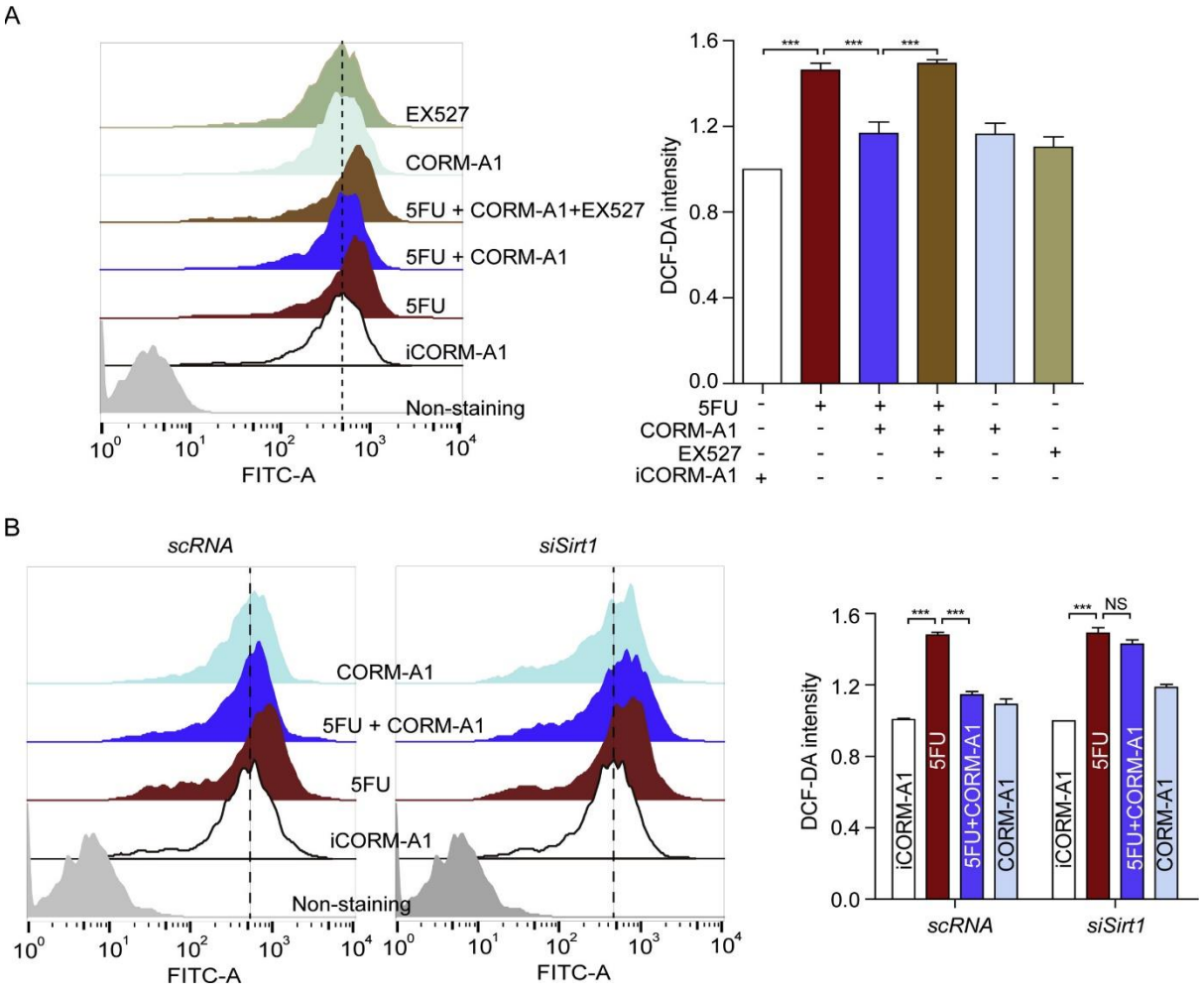

Fig. 10. SIRT1 is critical for the antioxidant effect of CO in WI-38 cells

(A) WI-38 cells were pretreated with EX527 (10 μM) for 1h followed by the administration of iCORM-A1 (40 μM) or CORM-A1 (40 μM) for 1h. Then, cells were treated with 5FU (70 μg/ml) for 4h and supplied with fresh medium. After 48 h incubation, the intracellular ROS was detected by staining with DCF-DA and examined with a flow cytometry (FACSCanto II). (B) WI-38 cells were transfected with *scRNA* and *siSirt1*. After 36h transfection, cells were treated with iCORM-A1 (40 μM) or CORM-A1 (40 μM) for 1h in the presence or absence of 5FU (70 μg/ml) for 48h. Then, the production of ROS was assessed by FACSCanto II. The fold change of mean fluorescence intensity is presented as mean ± SD (n = 3). ***$p < 0.001$, NS: not significant.

SIRT1 is associated with CO-induced SG assembly in 5FU-mediated cellular senescence

Our previous study demonstrated that CO induced the assembly of SGs via the PERK-eIF2α signaling pathway [22]. Thus, to investigate whether CO can promote SGs formation in 5FU-elicited endothelial senescence, we detected the SGs formation by immunofluorescence using anti-TIA-1 and-G3BP1 antibodies. Our results showed that 5FU administration slightly, but not significantly, increased the assembly of SGs, whereas the pretreatment with CORM-A1 in the presence of 5FU significantly increased the formation of SGs in HUVEC cells (Fig. 11A and B). Thapsigargin (Tg) is a well-known ER stress inducer that can increase the assembly of SGs owing to the activation of an integrated stress response [39]. Therefore, as a positive control, we treated HUVEC cells with a low dose of Tg (200 nM) for 40min to assess the levels of SGs assembly (Fig. 11A and B). A previous study reported that in response to stress, *C. elegans* SIR-2.4 and its mammalian orthologue SIRT6 localize to cytoplasmic SGs, interact with various SG components, and induce their assembly [40]. To investigate whether CO-induced SIRT1 is associated with SGs assembly, HUVECs were transfected with *siSirt1*. As shown in Fig.11C, CO-induced SIRT1 is required in SGs assembly. Here, we suggested that besides the PERK-eIF2α signaling pathway [22], SIRT1 might be a novel factor involved in CO-mediated SGs formation. Taken together, our findings support the hypothesis that CO can increase the formation of SGs in 5FU-mediated cellular senescence, which might be involved in SIRT1 activation.

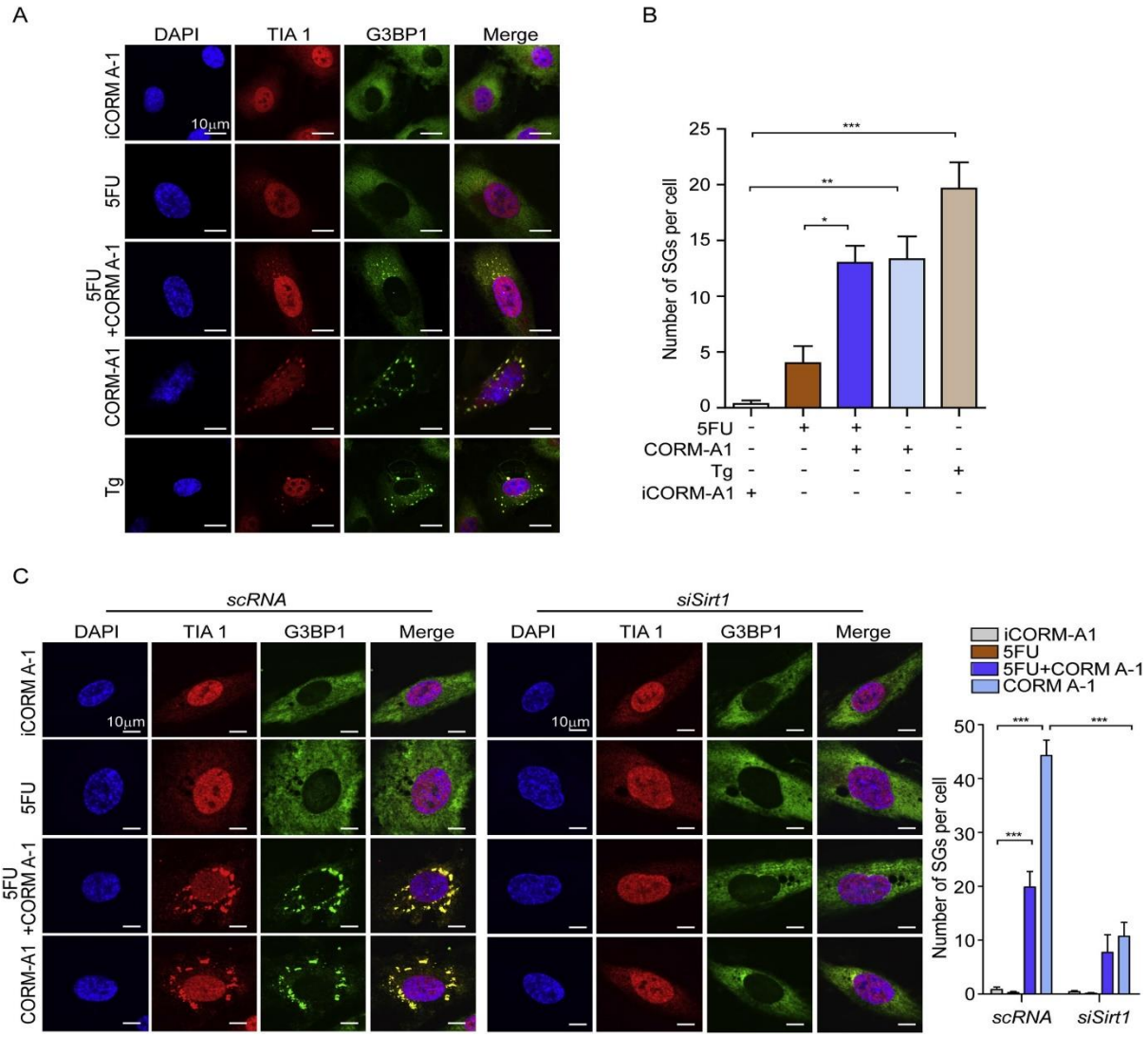

Fig. 11. SIRT1 is associated with CO-induced SG assembly in 5FU-mediated senescence

(A and B) HUVEC cells were treated with iCORM-A1 (40 μM) and CORM- A1 (40 μM) for 1h followed by the stimulation of 5FU (70 μg/ml). (C) HUVEC cells were transfected with *scRNA* and *siSirt1*. And then cells were treated with iCORM-A1 (40 μM) or CORM-A1 (40 μM) for 1h followed by the stimulation of 5FU (70 μg/ml). After a 4h-treatment with 5FU, cells were changed into fresh media, and were incubated for another 72 h to induce DNA damage-mediated premature cellular senescence. The assembly of SGs was observed by immunofluorescence using anti-TIA-1 and anti-G3BP1 antibodies. As a positive control,

HUVEC cells were treated with 200 nM thapsigargin (Tg) for 40min to assess the levels of SGs formation. Scale bars represent 10μm. Quantification from immunofluorescence images were achieved by counting the TIA-1 and G3BP1-positive granules per cell. Data were expressed as mean ± SD (n= 3 per group). One-way ANOVA with Tukey's post hoc tests was performed; *$p < 0.05$, **$p < 0.01$, and ***$p < 0.001$.

Schematic diagram of proposed pathway.

Our results suggest that CO alleviates the endothelial senescence induced by 5FU through the SIRT1 activation (Fig. 12). Therefore, CO might contribute to cellular therapies for vascular diseases.

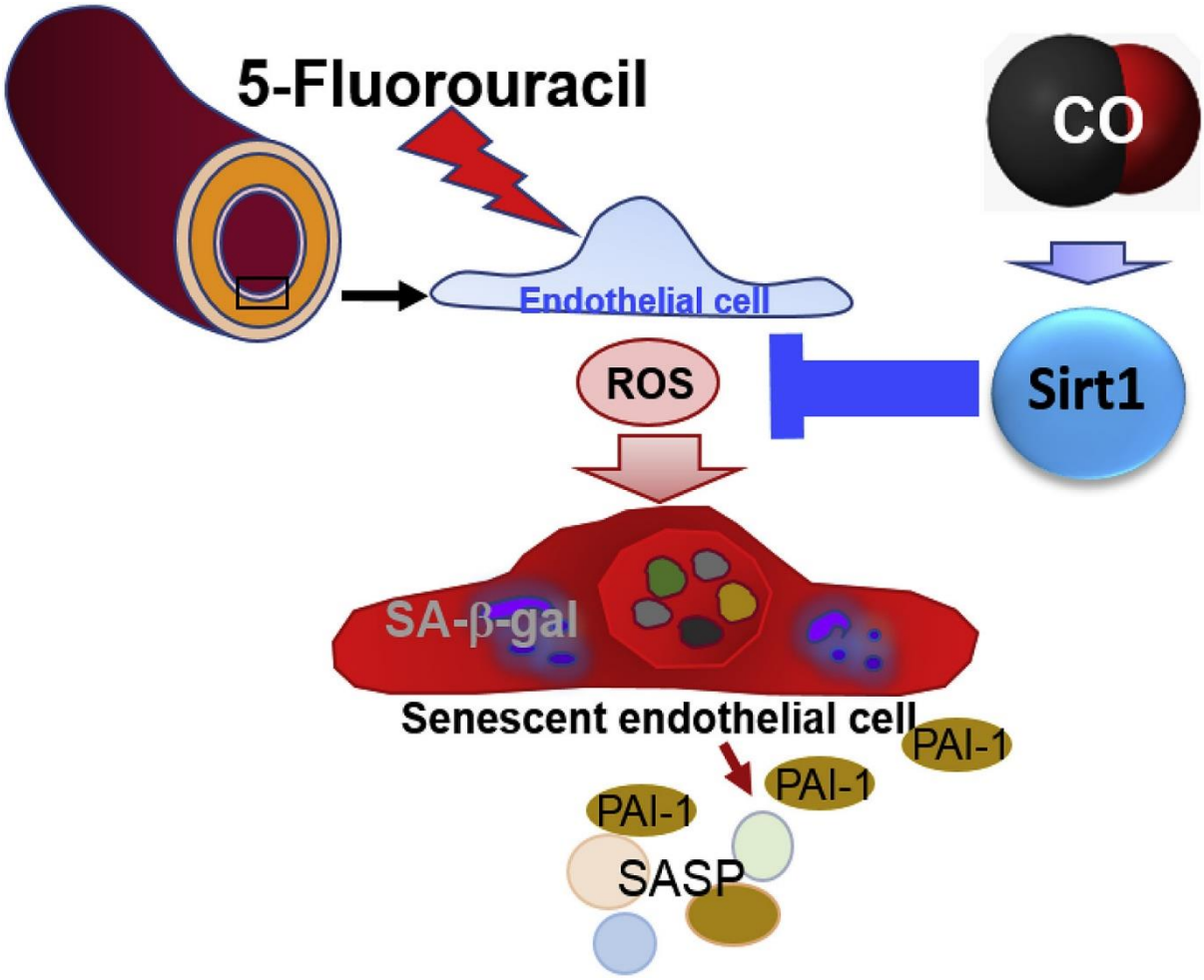

Fig. 12. Schematic diagram of proposed pathway.

5FU elicits the senescence of HUVECs by the generation of ROS. CORM-A1 prevents the 5FU-induced senescence in HUVECs via SIRT1 activation.

I-V. DISCUSSION

The present study showed that CO could prevent endothelial senescence induced by 5FU. Previously, researchers have reported the protective effects of CO on endothelial dysfunction [41–43]. However, the underlying mechanisms of this type of CO protective benefit have remained elusive. Endothelial senescence might be induced by endothelial dysfunction [44] and is one side-effect of 5FU use [45]. Therefore, we hypothesized that CO also plays a highly important role in preventing endothelial senescence induced by 5FU. In the present study, 5FU induced the senescence of HUVECs, which is consistent with the results of previous studies [4]. Additionally, sera from patients receiving a prodrug of 5FU caused endothelial cell senescence [4]. Furthermore, 5FU induced the senescence of WI-38 fibroblast cells, and we also found that CO prevented 5FU-induced senescence in WI-38 cells. Emerging evidence shows that one of the features of senescent fibroblasts is increased vascular endothelial growth factor expression, and senescent fibroblasts can stimulate cultured HUVECs to intrude into a basement membrane [46].

To detect whether 5FU induces senescence successfully, we investigated several senescence-associated factors. Lysosomal content increased in the senescent cells, which is often detected as high SA-β-gal activity [47]. The cyclin-dependent kinase inhibitor p21 has already been identified as being associated with endothelial senescence, as it can lead to the inhibition of the cyclin E-CDK2 complex [2]. SASP is another characteristic feature of cellular senescence [27]. Among the SASPs, PAI-1 and TNF-α have previously been shown to be enhanced in senescent endothelial cells [33,34]. In the present study, the SA-β -gal activity and p21, PAI-1, and TNF-α expression induced by 5FU was attenuated by CORM-A1 treatment.

These findings support our hypothesis that CO confers protection from endothelial senescence induced by 5FU.

ROS generation is another feature of endothelial senescence [48] and, because of the dysfunctional mitochondria accumulation, the senescent cell always exhibits high levels of ROS [47]. Recently, studies have demonstrated the role of oxidative stress caused by ROS in senescence [49]. Oxidative stress might damage DNA and proteins and induce cellular senescence [50]. Furthermore, HO-1 as an antioxidant protein ameliorates oxidative stress induced endothelial senescence [1]. We explored intracellular ROS generation and found that 5FU enhanced ROS generation, which is consistent with results from other studies [51], and this upregulation was decreased by the CO treatment. And we suggested that CO could prevent 5FU-induced senescence by increasing anti-oxidative activity, which produced the same result as treatment with the ROS scavenger, NAC (Fig.5-6). Therefore, we suggest that CO improves endothelial senescence by increasing HO-1. In addition to HO-1, CO increased the levels of eNOS and SIRT1 in endothelial cells (Fig.8). SIRT1 also is a crucial regulator of cell senescence [9], and we have previously reported that CO activates SIRT1 by inhibiting miR34a [29]. The NO generated by eNOS can protect cells from oxidative stress and delay endothelial cellular senescence [52,53]. The eNOS was activated by CO-releasing molecules or CO gas through intracellular calcium release and Akt phosphorylation [54]. Moreover, SIRT1 interacts with the vascular eNOS/NO system [55] and regulates vascular angiogenesis and senescence [56]. We found that SIRT1 activation by CO protects endothelial cells from 5FU-induced senescence. Moreover, CO-derived downregulation of SASP was involved in antioxidation and SIRT1 activity (Fig.9). In response to a variety of harmful stimuli, including heat, hyperosmolarity and oxidative conditions, eukaryotic cells will transiently turn off protein

synthesis, and enhance the assembly of SGs in the cytoplasm to control energy expenditure for the repair of stress-induced damage [21,57,58]. On the other hand, the formation of SGs can mediate the inhibition of cellular senescence, which is associated with the sequestration of PAI-1, a component of SASP [59]. Moreover, CO can induce the assembly of SGs through the PERK-eIF2α signaling pathway, which is a part of an integrated stress response [22]. However, whether CO can promote the formation of SGs in premature endothelial senescence remains undefined. Our study showed that CO induced the formation of SGs in HUVECs, and the SIRT1 inhibitor, EX527, blocked this effect of CO.

Our results suggest that CO alleviates the endothelial senescence induced by 5FU through the SIRT1 activation (Fig.12). Therefore, CO might contribute to cellular therapies for vascular diseases.

PART Ⅱ

TTP activation by CO ameliorates ALI via inhibition of SARM1-dependent ferroptosis

II-I. ABSTRACT

Ferroptosis, an iron-dependent form of programmed cell death, plays an important role during Acute lung injury (ALI). ALI is defined as a common life-threatening disease caused by several factors, including oxidative stress, inflammation, and cell death. Ferroptosis as a newly recognized cell death, the regulated mechanism of ferroptosis in ALI remains largely elusive. Carbon monoxide (CO) has been reported to have antioxidative, anti-apoptotic, and anti-inflammatory properties. We have previously established a protective role of carbon monoxide (CO) in ALI via inhibiting inflammatory responses through tristetraprolin (TTP) upregulation. Here, we further confirmed the beneficial effect of CO in ALI, we measured cell viability, lipid ROS generation and the mRNA levels of prostaglandin-endoperoxide synthase 2 (PTGS2) as well as sterile alpha and Toll/interleukin-1 receptor motif-containing 1(SARM1) in human lung epithelial cells A549 cells and mouse lung epithelial cell line MLE12 cells for in vitro experiments. We also used $TTP^{+/+}$ and $TTP^{-/-}$ mouse lung tissue for PTGS2 and SARM1 mRNA expression measurement for in vivo experiment. We found that LPS treatment induced lipid ROS generation, upregulation of PTGS2 level as well as SARM1 expression and downregulation of the cell viability while was restored by CO-releasing molecules-2 (CORM 2) treatment. Additionally, TTP activation triggered by CORM2 treatment attenuated SARM1 and PTGS2 level induced by LPS. Furthermore, TTP deficiency abolished the PTGS2 and SARM1 downregulation induced by CO. Our results showed the mechanism that TTP activation by CO ameliorates SARM1-dependent ferroptosis. We identified SARM1, one of NAD-consuming enzymes, can be degraded by TTP resulted in inhibition of lipid ROS generation and downregulation of PTGS2, leading to ameliorate ferroptosis. Thus, the crosstalk

between TTP and SARM1 provides a mechanism of control the resolution of inflammation and cell death in ALI.

II-II. INTRODUCTION

Acute lung injury (ALI) is a prevalent and critical life-threatening disorder affecting more than 200,000 people in the US each year, with approximately 75,000 deaths,[60] making it an important cause of high rates of morbidity and mortality among patients with numerous medical conditions. As a less severe form of acute respiratory distress syndrome (ARDS),which is a major cause of respiratory failure and one of the most challenging clinical conditions, ALI is characterized by the rapid and intense inflammatory response resulting in the accumulation of pulmonary neutrophils, interstitial edema, arterial hypoxemia, which damage the vascular endothelium and alveolar epithelium in the lung tissues**,** thus diminishing lung function.[61] It is currently reported that ALI may be caused by oxidative stress, inflammation, and cell death[62-64], but its pathogenesis is still unclear.

In recent years, an increasing number of ALI intervention strategies have been noticed that ultimately converge on ferroptosis. [65-66] Ferroptosis is an iron-dependent form of programmed cell death characterized by the accumulation of lipid hydroperoxides to lethal levels.[67] The term ferroptosis was first found by Dixon et al. in RAS mutant tumor cells treated with erastin in 2012.[68] Glutathione (GSH) which is the essential substrate for glutathione peroxide enzyme 4 (GPX4) to degrade phospholipid hydroperoxide (PLOOH), the depletion of GSH is one of the key events in ferroptosis. The cystine/glutamate antiporter System Xc-, which consists of SLC3A2 (solute carrier family 3 member 2) and SLC7A11 (solute carrier family 7 member 11) is an amino acid transporter that transports extracellular cystine and intracellular glutamate at a ratio of 1:1 to produce GSH. The utilization of GSH depends on the key enzyme GPX4. Inhibition of GPX4 through depletion of GSH with erastin,

or with the direct GPX4 inhibitor (1S,3R)-RSL3 (hereafter referred to as RSL3) , which can covalently bind to the active site Sec of GPX4 and directly inhibit the activity of GPX4 ultimately results in overwhelming lipid peroxidation that causes ferroptosis.[67]

Meanwhile, SARM1 (sterile alpha and Toll/interleukin-1 receptor motif-containing 1), the founding member of a family of Toll/interleukin-1 receptor (TIR)-domain containing enzymes that cleaves the essential metabolite nicotinamide adenine dinucleotide (NAD^+) into nicotinamide (NAM) and adenosine diphosphate ribose (ADPR), is a key executioner of cell death due to the severe depletion of NAD^+ [69]. Furthermore, SARM1 has recently been shown to have a role in mammalian neuronal-cell death in response to infection and injury and regulate inflammasome-dependent cytokine release and cell death in macrophages.[70] We considered whether SARM would regulate ferroptosis in ALI.

Tristetraprolin (TTP, encoded by Ttp, also known as Zfp36) is an RNA binding and RNA-destabilizing protein that bind directly to AU-rich elements (AREs) in the 3 ′-untranslated region (UTR) of their target mRNAs and promote the removal of the polyA tail, followed by complete mRNA decay. By destabilizing their target mRNAs, TTP can promotes degradation of a number of inflammatory mediators, such as TNF-a, IL-2, IL-3 and IL-6.[71] In addition to the anti-inflammatory effects of TTP, TTP also as players in cellular iron homeostasis that regulate mRNA stability of TfR1 and iron-containing genes. TTP can be strongly induced by iron chelation, promotes downregulation of iron-requiring genes in both mammalian and yeast cells, and modulates survival in low-iron states.[72] Because we have previously established a protective role of carbon monoxide (CO) in ALI, [71] which is an inducer of TTP activation, can inhibit inflammatory responses through TTP upregulation. Furthermore, in our recent

study, we demonstrated that TTP activation induced by CO ameliorates the inflammatory response and promotes autophagic bacterial clearance in sepsis-induced ALI through CD38 degradation, an NAD^+ depleting enzyme, leading to a rise of NAD^+ levels, and activation of Sirt1.[73] We considered whether SARM1 which also acts as an NAD-consuming enzyme would be degraded by TTP, and then regulate inflammation and ferroptosis in ALI.

In the current study, we sought to identify the role of SARM1 in ferroptosis in ALI. We found that TTP activation by CO ameliorates ALI via inhibition of SARM1-dependent ferroptosis. We conclude that the nexus of TTP and SARM1 provides a mechanism of control the resolution of inflammation and cell death in ALI.

II-III. MATERIALS AND METHODS

1. Reagents

Lipopolysaccharide (LPS), carbon monoxide-releasing molecule- (CORM-) 2, were purchased from Sigma-Aldrich, (St. Louis, MO, USA). Ferrostatin-1 was purchased from Selleckchen, siRNA against TTP was from Santa Cruz Biotechnology (Santa Cruz, CA).

2. Animals

All mice in this study were on pure C57BL/6 background. *Ttp*$^{-/-}$ male mice, in C57BL/6 background, were provided by Dr. Perry J. Blackshear (Laboratory of Signal Transduction, National Institute of Environmental Health Sciences, USA). Animal studies were approved by the University of Ulsan Animal Care and Use Committee (Reference number HTC-14–030). All mice were maintained under specific pathogen-free conditions at 18-24 ℃ and 40%–70% humidity, with a 12 h light-dark cycle.

3. Cell Culture

Human lung epithelial A549 cells (KCLB, Seoul, Korea) were cultured in RPMI 1640 medium (Gibco, Grand Island, NY, USA), containing 10% FBS and 1% penicillin-streptomycin, at 37°C in humidified incubators containing an atmosphere of 5% CO_2. Mouse lung epithelial MLE12 cells were cultured in a humidified incubator maintained at 37° C and 5% CO2 in Dulbecco's modified Eagle's medium (11965, Gibco, USA) containing 10% fetal bovine serum (0500, Gibco, USA), and 1% penicillin-streptomycin.

4. LPS-induced ALI and CO inhalation

For in vivo experiments 10-week-old *Ttp*$^{+/+}$ and *Ttp*$^{-/-}$ male mice were randomly assigned into three groups (10 mice in each group), including Vehicle, LPS, LPS+CO gas. Mice were exposed to CO gas (250 ppm) for 4 h per day in an exposure chamber (LB Science, Daejeon, Korea) for 7 days. Then mice were challenged with LPS (25mg/kg), and then mice were sacrificed after 24 h. Lung tissues were harvested to measure the expression of SARM1 as well as PTGS2 by RT-PCR.

5. RNA Isolation and Reverse Transcription-Polymerase Chain Reaction

Total RNA was isolated from A549 cells, MLE12 cells and lung tissues using TRIzol reagent (Invitrogen). 2μg of total RNA was used to synthesize cDNA by using M-MLV reverse transcriptase (Promega). The synthesized cDNA was subject to PCR-based amplification. The following primers were mouse GAPDH (F-AGGCCGGTGCTGAGTATGTC, R-TGCCTGCTTCACCTTCT), mouse SARM1 (F-CGCTGCCCTGTACTGGAGG, R-CTTCAGGCTGGCCAGCT), mouse TTP (F-CTCTGCCATCGAGAGCC, R-GATGGAGTCCGAGTTTATGTTCC) m18S (F-GGGAGCCTGAGAAACGGC, R-GGGTCGGGAGTGGGTAATTT), mouse PTGS2 (F-TTCCAAATGTCAAAACCGT R-AGTCCGGGTACAGTCACACTT), human SARM1 (F-ATCTTGGAGCACATGTTCA, R-CTGCGCGCTTCTCTACCAT), human GAPDH (F-CAATGACCCCTTCATTGACCTC, R-AGCATCGCCCCACTTGATT). To perform real-time quantitative PCR (RT-qPCR), the synthesized cDNA was amplified with SYBR Green qPCR Master Mix (2x, USB Production; Affymetrix) on an ABI 7500 Fast Real-Time PCR System (Applied Biosystems, Carlsbad, CA). The following RT-qPCR primers were mouse GAPDH (F-

GGGAAGCCCATCACCATCT, R-CGGCCTCACCCCATTTG), mouse SARM1 (F-CGCTGCCCTGTACTGGAGG, R-CTTCAGGCTGGCCAGCT).

6. Cell viability assays

(The WST-8 (QuantiMax™-Cell viability assay kit) was used to analyze cell viability according to the manufacturer's instructions. A549 cells (1×10^4/well) were plated onto 96-well plates. All assays were performed in triplicate. Cells in each well were suspended in 100μL fresh medium containing the various treatment and then seeded. After treatment, WST-8 (10 μL/well) was added for 4h of additional incubation, and the absorbance was measured at 450nm.

7. Dual Luciferase Assay

For dual luciferase assay, A549 cells were grown in a 96-well plate, and then cells were co-transfected with SARM1 3′-UTR construct and pcDNA6/V5-TTP (0.1 μg or 0.5 μg). After 72 h, treated cells were lysed with passive lysis buffer (Promega, Fitchburg, WI, USA) and mixed with luciferase assay reagents (Promega). The chemiluminescent signal was detected using a SpectraMax L Microplate reader (Molecular Devices, Sunnyvale, CA). Firefly luciferase was normalized to Renilla luciferase in each sample.

8. Lipid ROS Measurement

To perform lipid ROS measurement by FACS, A549 cells were pretreated with CORM2 (20 μM) or with Fer-1 (2μM) for 1h, respectively, and then stimulated with LPS (10 μg/ml) for

an additional 24 h. After treatment, cells were stained with C-11 BODIPY dye (5 μM) for 30 min and then washed four times with PBS. Lipid ROS was assessed by using flow cytometry with a fluorescence-activated cell sorter (FACSCanto II), and data was analyzed by FlowJo V10 software (Tree Star Inc., San Carlos, CA).

9. Statistical Analysis

For statistical comparison, all data were presented as mean ± SD (n =3). The comparison among all experimental groups were made by One-way ANOVA with Tukey's post hoc tests, and all statistical analysis were assessed by GraphPad Prism software version 5.03 (SanDiego, CA). The changes among groups with probability values of $p \leq 0.05$ were considered statically significant.

II-IV. RESULTS

CO inhibits LPS-induced ferroptosis in lung epithelial cells.

Given the protective role of CO [71] and the important role of ferroptosis in ALI [65-66], we firstly explored the effect of CO in lung epithelial cells. To investigate the effect of CO on ferroptosis in lung epithelial cells, we treated LPS (10μg/ml) for 24h to induce the ferroptosis [74] in A549 lung epithelial cells. LPS treatment significantly decreased the cell viability and restored by the CORM2 treatment and ferroptosis inhibitor ferrostatin 1 (Fer-1) treatment (Figure 13A). Next, we also measured the biomarker of ferroptosis prostaglandin-endoperoxide synthase 2 (PTGS2) mRNA level by RT-PCR, LPS treatment robustly upregulated the PTGS2 mRNA level while abolished by CORM2 as well as ferrostatin 1 treatment (Figure 13B and C). These data suggested that CO inhibits LPS-induced ferroptosis in lung epithelial cells.

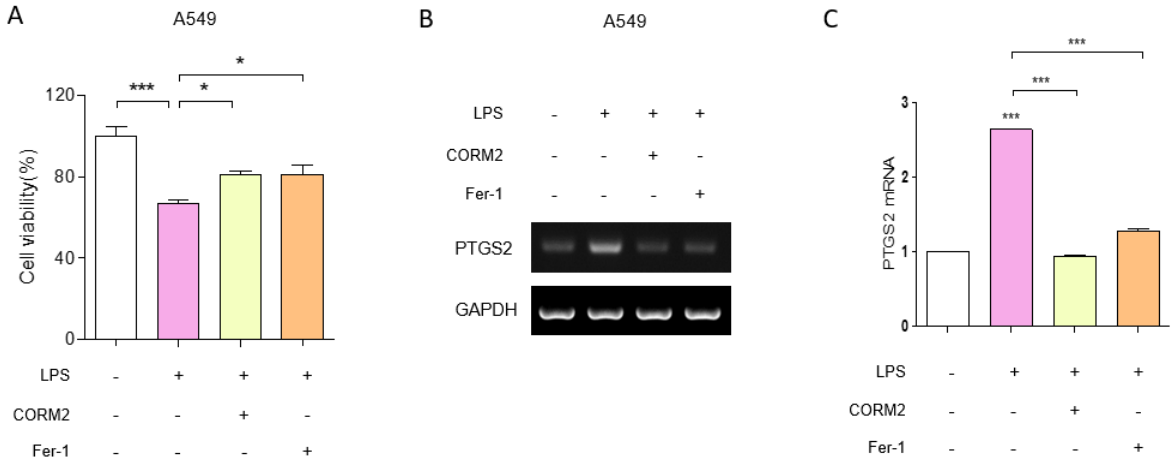

Figure 13. CO inhibits LPS-induced ferroptosis in lung epithelial cells.

(A)lung epithelial cell A549 cell viability after treatment LPS(10μg/ml) for 24h ,CORM2

(20μM) and Fer-1(2μM) pretreatment 1h, was evaluated by Quanti-max™ WST-8 cell viability assay kit. (B) PTGS2 mRNA level measured by RT-PCR in A549 cells treated with LPS (10μg/ml) for 24h, CORM2 (20μM) and Fer-1(2μM) pretreatment 1h (C) Quantification of PTGS2/GAPDH is shown in the panel of (C) (n = 3). Data were presented as mean±SD (n=3). *, P<0.05; **, P<0.01; ***, P<0.001; NS, statistically not significant.

CO resists lipid peroxidation in LPS-treated lung epithelial cells.

Ferroptosis is an iron-dependent oxidative form of cell death related to increased lipid peroxidation and inadequate capacity to clear off lipid peroxides [75]. Next, we investigated the lipid ROS level in A549 cells under the treatment of LPS (10μg/ml) for 24h, pretreated with CORM2 (20μM) and Fer-1(2μM) for 1h. As shown in FACS result, compared to control group LPS increased the lipid ROS level, but the upregulation of the lipid ROS level induced by LPS was decreased by CORM2 and Fer-1 treatment (Figure 14A-B) Hence, these results suggest that CO inhibits lipid ROS generation in LPS-induced ferroptosis in A549 lung epithelial cells.

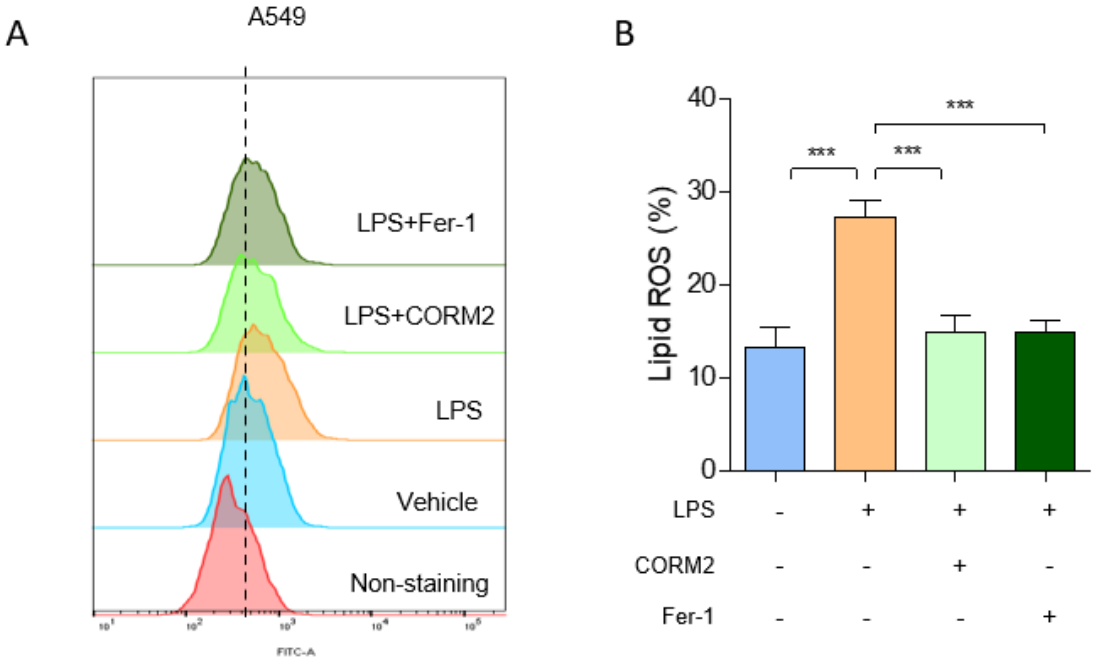

Figure 14. CO resists lipid peroxidation in LPS-treated lung epithelial cells.

(A) Lipid peroxidation levels of A549 cells pre-incubated with CORM2 (20μM) Fer-1(2μM)

for 1h were treated with LPS (10μg/ml) as indicated for 24h. (B) Quantification of lipid peroxidation levels are shown as in (B). Data were presented as mean±SD (n=3). *, P<0.05; **, P<0.01; ***, P<0.001; NS, statistically not significant.

SARM1 involves in LPS-induced ferroptosis.

Given the role of SARM in regulating neuronal-cell death [76] and non-apoptotic cell death [77]. In addition, SARM1 has recently been shown to regulate inflammasome-dependent cytokine release and cell death in macrophages.[70], next we examined whether SARM1 would regulate ferroptosis in the context of LPS-induced ALI. Thus, A549 cells primed with LPS (10μg/ml) for 24h, SARM1 mRNA level as measured by RT-PCR, which was significantly increased in dose-dependent manner compared to control group (Figure 15A and B). Altogether, these data indicating that SARM1 plays an important role in LPS-induced ferroptosis.

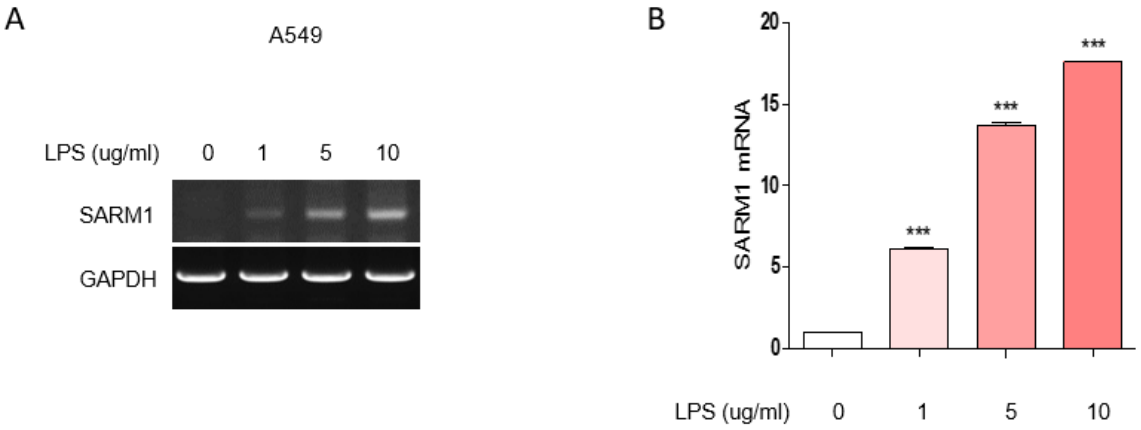

Figure 15. SARM1 involves in LPS-induced ferroptosis.

(A) SARM1 mRNA level measured by RT-PCR in A549 cells treated with LPS (0,1,5,10 μg/ml) for 24h (B) Quantification of SARM1/GAPDH is shown in the panel of (B) (n = 3). Data were presented as mean±SD (n=3). *, P<0.05; **, P<0.01; ***, P<0.001; NS, statistically not significant.

TTP induces SARM1 degradation.

The data thus far demonstrated that CO inhibits LPS-induced ferroptosis in lung epithelial cells and SARM1 upregulated in LPS-induced ferroptosis. Additionally, we previously reported that TTP activation induced by CO reduces the inflammatory response and promotes autophagic bacterial clearance in sepsis-induced ALI through CD38 degradation, an NAD^+ depleting enzyme, leading to a rise of NAD^+ levels, and activation of Sirt1.[73] We next examined whether SARM1 which also acts as an NAD-consuming enzyme would be degraded by TTP in LPS-induced ferroptosis. SARM1 mRNA expression markedly increased in $TTP^{-/-}$mouse lung tissue compared with the $TTP^{+/+}$ mouse lung tissue measured by RT-PCR (Figure 16A) As TTP is an RNA binding and RNA-destabilizing protein can bind directly to AU-rich elements (AREs) in the 3′-UTRs of their target mRNAs and promote the removal of the poly-A tail, followed by complete mRNA decay.[71] So we explored the SARM1 3′-UTR activity in A549 cells transfected with pcDNA6/V5-TTP by dual luciferase assay. As shown in Figure16B, SARM1 3′-UTR luciferase activity robustly decreased in TTP overexpressing cells in a dose-dependent manner compared to control group, suggesting that the mechanism whereby TTP negatively regulated SARM1 involves in CO prevent from LPS-induced ferroptosis.

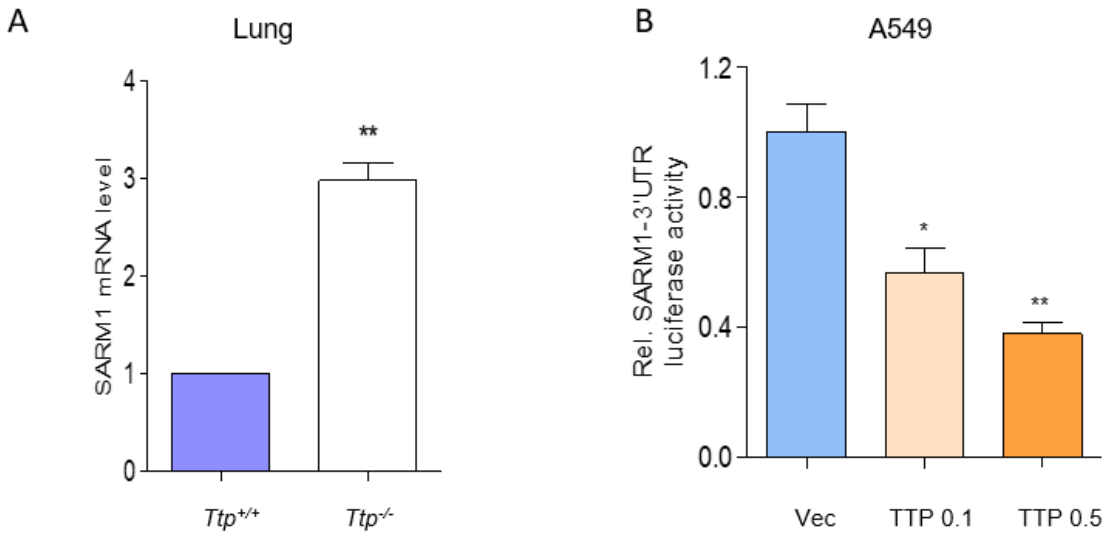

Figure 16.TTP induces SARM1 degradation.

(A)SARM1 mRNA level measured by qRT-PCR in *TTP*$^{+/+}$ and *TTP*$^{-/-}$mouse lung tissue. (B) Luciferase activity in A549 cells co-transfected with SARM1 3′-UTR construct and pcDNA6/V5-TTP (0.1 μg or 0.5 μg) (n = 3). Data were presented as mean±SD (n=3). **, P<0.01; ***, P<0.001; NS, statistically not significant.

TTP-regulated SARM1 degradation protects against LPS-induced ferroptosis in vitro

According to the results as we mentioned until now, we hypothesized that NAD-consuming enzyme SARM1 which also has AU-rich element also can be degraded by TTP activation induced by CO, and then prevent from the ferroptosis in ALI. Thus, we treated mouse lung epithelial cell line MLE12 cells with LPS 10 μg/ml for 24h, and then measured the mRNA expression of the SARM1 in TTP overexpressing MLE12 cells transfected with V5-TTP as well as TTP deleted cells using siRNA transfection in lung epithelial cell by RT-PCR. As expected, LPS significantly increased the SARM1 level in the presence of TTP and more incresed by TTP deletion using siRNA transfection. (Figures 17A and B). In the other hand, LPS significantly increased SARM1 mRNA level while TTP overexpressing markedly decreased SARM1 mRNA level followed by LPS treatment (Figures 17C and D). Taken together, these data suggested that TTP-regulated SARM1 degradation protects against LPS-induced ferroptosis in vitro.

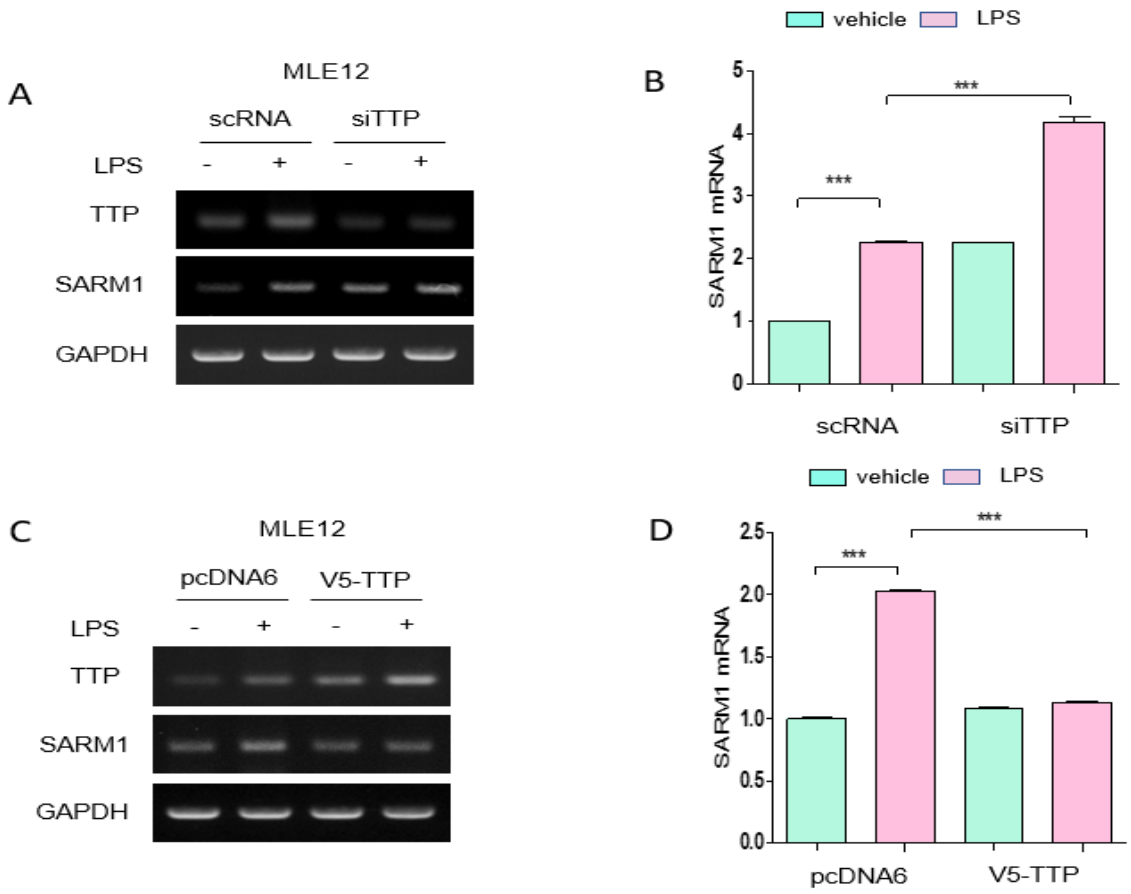

Figure 17.TTP regulated-SARM1 degradation protects against LPS-induced ferroptosis in vitro

(A)SARM1 mRNA level measured by RT-PCR in MLE12 cells treated with LPS 10μg/ml for 24h transfection with scramble RNA (*scRNA*) or siRNA against TTP (*siTTP*) (B) Quantification of SARM1/GAPDH is shown in the panel of (B) (n = 3). (C) SARM1 mRNA level in MLE12 cells treated with LPS 10ug/ml for 24h transfected with pcDNA6 or TTP-V5 (D) Quantification of SARM1/GAPDH is shown in the panel of (D) (n = 3). Data were presented as mean±SD (n=3). **, P<0.01; ***, P<0.001; NS, statistically not significant.

TTP-mediated SARM1 degradation protects against LPS-induced ferroptosis in vivo.

Finally, to confirm this mechanism in vivo, we detected SARM1 an PTGS2 level in *TTP*$^{+/+}$ and *TTP*$^{-/-}$mouse lung tissue. As expected, LPS injection significantly increased SARM1 and PTGS2 expression but decreased by CO inhalation in *TTP*$^{+/+}$ mouse, while not in *TTP*$^{-/-}$mouse. In *TTP*$^{-/-}$mouse, CO had no effect on the upregulation SARM1 and PTGS2 level induced by LPS. (Figures18A-C). Thus, these data confirmed that TTP mediated-SARM1 degradation protects against LPS-induced ferroptosis in vivo.

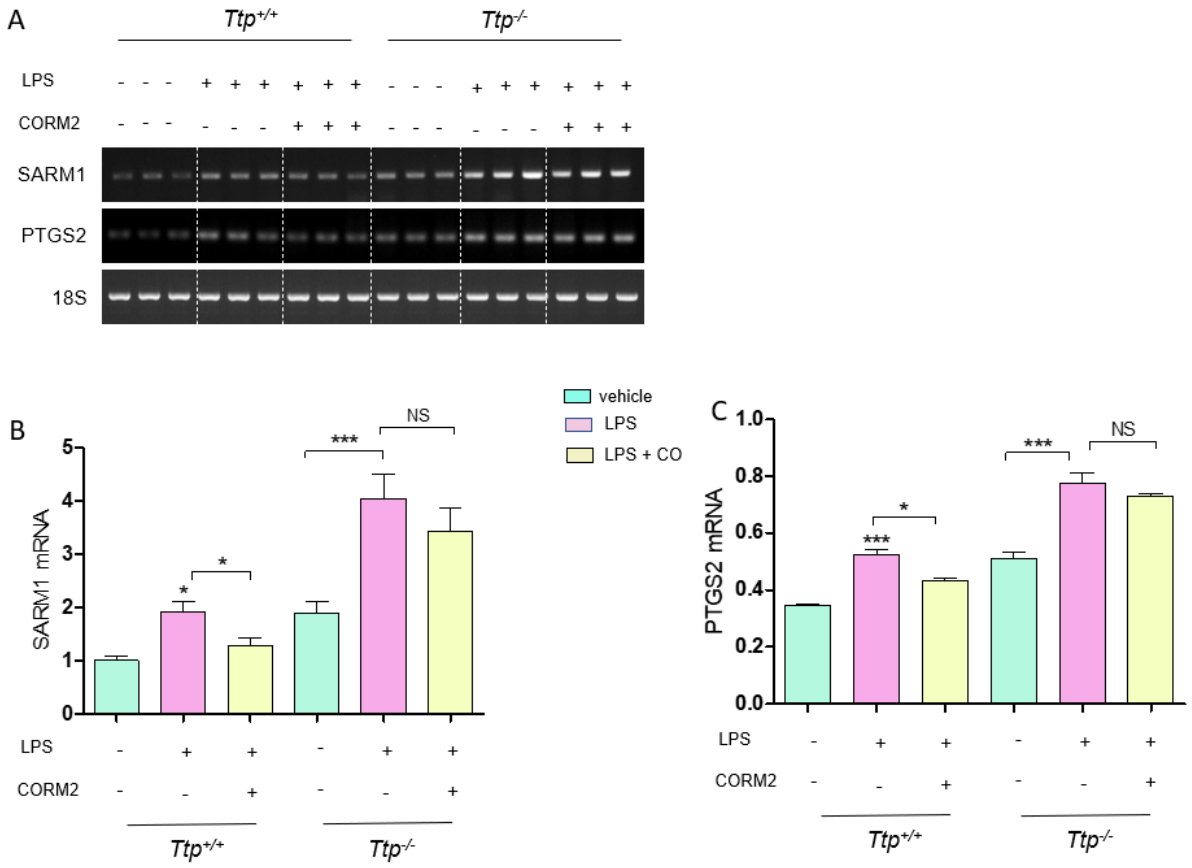

Figure 18.TTP mediated-SARM1 degradation protects against LPS-induced ferroptosis in vivo

(A)The mRNA levels of SARM1 and PTGS2 in lung tissues from *Ttp*+/+ and *TTP*$^{-/-}$ male mice (n=3 per group) in the presence of CO inhalation (250 ppm/4 h/day for 7 days). (B-C) Quantification of SARM1 (B) and PTGS2 (C) is shown in panels (n = 3). Data were expressed as mean ± SD. *p < 0.05; **p < 0.01; ***p < 0.001; NS, not significant.

II-V. DISCUSSION

The data presented here indicate that TTP-mediated -SARM1 degradation has a protective role in regulating cell fate after LPS administration. Specifically, we have shown that: (1) SARM1, a mammalian TIR-domain-containing protein, positively regulates the LPS induced ferroptosis. (2) In response to TTP activation, SARM1 expression and SARM1 3′-UTR luciferase activity markedly decreased leading to ferroptosis resistance, confirming the protect role of TTP in ferroptosis in lung epithelial cells. Consistent with that, other investigators showed that RNA-binding protein TTP protects against ferroptosis by regulating autophagy signaling pathway in hepatic stellate cells [78] (3)we identified PTGS2, the biomarker of ferroptosis as a target gene is decreased by TTP activator CO. (4) lipid ROS contributes to LPS-induced ferroptosis and was inhibited by CO, which can further confirm the protective role of CO in LPS-induced ferroptosis, as lipid ROS inducing lipid peroxidation plays a critical role in ferroptosis.

Previously, we have reported the protective effects of TTP in ALI [71,73]. Additionally, ferroptosis is a newly recognized type of iron-dependent programmed cell death [79] that including lipid peroxidation as well as Fe and ROS accumulation. Emerging evidence indicate a strong correlation between ALI and ferroptosis [65-66]. We found that CO inhibits ferroptosis in ALI targeting at the downregulation of PTGS2 (Figure13). PTGS2, also known as cyclooxygenase-2 (Cox-2), plays an important role in prostaglandin biosynthesis, and acts both as a peroxidase and as a dioxygenase [80,81]. which is usually considered as a biomarker of ferroptosis because of it oxidize lysophospholipids property [82]. We showed that PTGS2 is involved in the process of ferroptosis because it was significantly upregulated after treatment

with LPS in lung epithelial cells (Figure13). This small molecule was shown to be specific inducers of ferroptotic cell death and ideal probes. [83] In our data, we showed that CO significantly reduced the upregulation of PTGS2 in LPS-induced ferroptosis (Figure13).

Lipid peroxidation is another feature of ferroptosis. Glutathione (GSH) is one of the most important components of the cell's antioxidant defenses, which consisting of glutamate, cysteine, and glycine. Among these three components the cysteine is critical in the reduction of oxidized intracellular components. Furthermore, GSH is an important step in preventing ferroptosis as it used by GPX4 to reduce lipid peroxides to their alcohol form [84]. GPX4 inhibition leads to upregulation of PTGS2 which is involved in the synthesis of prostaglandins. PTGS2 is a marker of increased lipid peroxidation and ferroptotic cell death [85], In our data, consist with downregulation of PTGS2 by CO treatment in LPS-induced ferroptosis, CO also significantly ameliorated lipid ROS level induced by LPS administration (Figure14).

SARM1, an NAD-utilizing enzyme, consists of three defined protein domains the ARM repeats, the two SAM domains, and the TIR domain [86]. Carty et al. identified both the SAM and TIR domains of SARM are required. to drive pyroptosis, a highly inflammatory form of lytic programmed cell death. They found that SARM clustered at the mitochondria oligomerize at the mitochondria after NLRP3 activation to facilitate MDP contributes to NLRP3-dependent pyroptosis [70]. Here, we firstly identified the role of SARM1 in ferroptosis, an iron-dependent programmed cell death. We found that LPS-induced ferroptosis in lung epithelial cells and lung tissue is SARM1-dependent and blocked by CO via the TTP activation-mediated SARM1 degradation (Figure18).

Taken together, these data have introduced a new insight of SARM1 in the ferroptosis in ALI. CO inhibits LPS-induced ferroptosis through TTP-regulated SARM1 degradation, Subsequently, SARM1 degradation leads to inhibition of lipid ROS, which prevents ferroptosis. Finally, TTP plays a crucial role in the resolution of SARM1-dependent ferroptosis in ALI. Our studies therefore identify the targets for ALI therapies aimed at modulating SARM1-dependent ferroptosis.

CONCLUSION

As we have discussed, CO has beneficial effect on both endothelial cell senescence and ALI. CO alleviates the endothelial senescence induced by 5FU through the SIRT1 activation. Additionally, CO inhibits LPS-induced ferroptosis in lung epithelial cells through TTP-regulated SARM1 degradation, Subsequently, SARM1 degradation leads to inhibition of lipid ROS, which prevents ferroptosis. Finally, TTP plays a crucial role in the resolution of SARM1-dependent ferroptosis in ALI. Our studies therefore identify the targets for ALI therapies aimed at modulating SARM1-dependent ferroptosis. Therefore, CO might contribute to cellular therapies for vascular diseases and ALI.

REFERENCES

[1] W. Luo, Y. Wang, H. Yang, C. Dai, H. Hong, J. Li, Z. Liu, Z. Guo, X. Chen, P. He, Z. Li, F. Li, J. Jiang, P. Liu, Z. Li, Heme oxygenase-1 ameliorates oxidative stress-induced endothelial senescence via regulating endothelial nitric oxide synthase activation and coupling, Aging (Albany NY) 10 (7) (2018) 1722–1744.

[2] J.D. Erusalimsky, Vascular endothelial senescence: from mechanisms to pathophysiology, J. Appl. Physiol. 106 (1) (1985) 326–332 2009.

[3] D. Cunningham, W. Atkin, H.J. Lenz, H.T. Lynch, B. Minsky, B. Nordlinger, N. Starling, Colorectal cancer, Lancet 375 (9719) (2010) 1030–1047.

[4] P. Altieri, R. Murialdo, C. Barisione, E. Lazzarini, S. Garibaldi, P. Fabbi, C. Ruggeri, S. Borile, F. Carbone, A. Armirotti, M. Canepa, A. Ballestrero, C. Brunelli, F. Montecucco, P. Ameri, P. Spallarossa, 5-fluorouracil causes endothelial cell senescence: potential protective role of glucagon-like peptide 1, Br. J. Pharmacol. 174 (21) (2017) 3713–3726.

[5] J. Tato-Costa, S. Casimiro, T. Pacheco, R. Pires, A. Fernandes, I. Alho, P. Pereira, P. Costa, H.B. Castelo, J. Ferreira, L. Costa, Therapy-induced cellular senescence induces epithelial-to-mesenchymal transition and increases invasiveness in rectal cancer, Clin. Colorectal Cancer 15 (2) (2016) 170–178 e3.

[6] W.K. Chen, Y.L. Tsai, M.A. Shibu, C.Y. Shen, S.N. Chang-Lee, R.J. Chen, C.H. Yao, B. Ban, W.W. Kuo, C.Y. Huang, Exercise training augments Sirt1-signaling and attenuates cardiac

inflammation in D-galactose induced-aging rats, Aging (Albany NY) 10 (12) (2018) 4166–4174.

[7] X. Bi, Q. Ye, D. Li, Q. Peng, Z. Wang, X. Wu, Y. Zhang, Q. Zhang, F. Jiang, Inhibition of nucleolar stress response by Sirt1: a potential mechanism of acetylation-independent regulation of p53 accumulation, Aging Cell 18 (2) (2019) e12900.

[8] S. Chung, H. Yao, S. Caito, J.W. Hwang, G. Arunachalam, I. Rahman, Regulation of SIRT1 in cellular functions: role of polyphenols, Arch. Biochem. Biophys. 501 (1) (2010) 79–90.

[9] Z.Z. Chong, Y.C. Shang, S. Wang, K. Maiese, SIRT1: new avenues of discovery for disorders of oxidative stress, Expert Opin. Ther. Targets 16 (2) (2012) 167–178.

[10] S. Moncada, M.W. Radomski, R.M. Palmer, Endothelium-derived relaxing factor. Identification as nitric oxide and role in the control of vascular tone and platelet function, Biochem. Pharmacol. 37 (13) (1988) 2495–2501.

[11] J. Dulak, J. Deshane, A. Jozkowicz, A. Agarwal, Heme oxygenase-1 and carbon monoxide in vascular pathobiology: focus on angiogenesis, Circulation 117 (2) (2008) 231–241.

[12] S.W. Ryter, J. Alam, A.M. Choi, Heme oxygenase-1/carbon monoxide: from basic science to therapeutic applications, Physiol. Rev. 86 (2) (2006) 583–650.

[13] R.F. Coburn, Mechanisms of carbon monoxide toxicity, Prev. Med. 8 (3) (1979) 310–322.

[14] Y. Chen, T.J. Cohen, Aggregation of the nucleic acid-binding protein TDP-43 occurs via distinct routes that are coordinated with stress granule formation, J. Biol. Chem. 294 (10) (2019) 3696–3706.

[15] H. Tourriere, K. Chebli, L. Zekri, B. Courselaud, J.M. Blanchard, E. Bertrand, J. Tazi, The RasGAP-associated endoribonuclease G3BP assembles stress granules, J. Cell Biol. 160 (6) (2003) 823–831.

[16] N. Kedersha, M.R. Cho, W. Li, P.W. Yacono, S. Chen, N. Gilks, D.E. Golan, P.Anderson, Dynamic shuttling of TIA-1 accompanies the recruitment of mRNA to mammalian stress granules, J. Cell Biol. 151 (6) (2000) 1257–1268.

[17] R. Mazroui, M.E. Huot, S. Tremblay, C. Filion, Y. Labelle, E.W. Khandjian, Trapping of messenger RNA by Fragile X Mental Retardation protein into cytoplasmic granules induces translation repression, Hum. Mol. Genet. 11 (24) (2002) 3007–3017.

[18] G. Stoecklin, T. Stubbs, N. Kedersha, S. Wax, W.F. Rigby, T.K. Blackwell, P. Anderson, MK2-induced tristetraprolin:14-3-3 complexes prevent stress granule association and ARE mRNA decay, EMBO J. 23 (6) (2004) 1313–1324.

[19] O. Moujaber, H. Mahboubi, M. Kodiha, M. Bouttier, K. Bednarz, R. Bakshi, J. White, L. Larose, I. Colmegna, U. Stochaj, Dissecting the molecular mechanisms that impair stress granule formation in aging cells, Biochim. Biophys. Acta Mol. Cell Res. 1864 (3) (2017) 475–486.

[20] X.J. Lian, I.E. Gallouzi, Oxidative stress increases the number of stress granules in senescent cells and triggers a rapid decrease in p21waf1/cip1 translation, J. Biol. Chem. 284 (13) (2009) 8877–8887.

[21] M.D. Panas, P. Ivanov, P. Anderson, Mechanistic insights into mammalian stress granule dynamics, J. Cell Biol. 215 (3) (2016) 313–323.

[22] Y. Chen, Y. Joe, J. Park, H.C. Song, U.H. Kim, H.T. Chung, Carbon monoxide induces the assembly of stress granule through the integrated stress response, Biochem. Biophys. Res. Commun. 512 (2) (2019) 289–294.

[23] R. Motterlini, P. Sawle, J. Hammad, S. Bains, R. Alberto, R. Foresti, C.J. Green, CORM A1: a new pharmacologically active carbon monoxide-releasing molecule, FASEB J. 19 (2) (2005) 284–286.

[24] B. van der Loo, M.J. Fenton, J.D. Erusalimsky, Cytochemical detection of a senescence-associated beta-galactosidase in endothelial and smooth muscle cells from human and rabbit blood vessels, Exp. Cell Res. 241 (2) (1998) 309–315.

[25] H.R. Seo, M.J. Choi, J.M. Choi, J.C. Ko, J.Y. Ko, E.J. Cho, Malvidin protects WI-38 human fibroblast cells against stress-induced premature senescence, J. Cancer Prev.21 (1) (2016) 32–40.

[26] F. Rodier, J. Campisi, Four faces of cellular senescence, J. Cell Biol. 192 (4) (2011)547–556.

[27] J.P. Coppe, C.K. Patil, F. Rodier, Y. Sun, D.P. Munoz, J. Goldstein, P.S. Nelson, P.Y. Desprez, J. Campisi, Senescence-associated secretory phenotypes reveal cell nonautonomous functions of oncogenic RAS and the p53 tumor suppressor, PloS Biol. 6 (12) (2008) 2853–2868.

[28] K.M. Kim, S.E. Park, M.S. Lee, K. Kim, Y.C. Park, Induction of heme oxygenase1 expression protects articular chondrocytes against cilostazol induced cellular senescence, Int. J. Mol. Med. 34 (5) (2014) 1335–1340.

[29] H.J. Kim, Y. Joe, J.K. Yu, Y. Chen, S.O. Jeong, N. Mani, G.J. Cho, H.O. Pae, S.W. Ryter, H.T. Chung, Carbon monoxide protects against hepatic ischemia/reperfusion injury by modulating the miR-34a/SIRT1 pathway, Biochim. Biophys. Acta 1852 (7) (2015) 1550–1559.

[30] H. Ota, M. Akishita, M. Eto, K. Iijima, M. Kaneki, Y. Ouchi, Sirt1 modulates premature senescence-like phenotype in human endothelial cells, J. Mol. Cell. Cardiol. 43 (5) (2007) 571–579.

[31] J.A. Maier, M. Statuto, G. Ragnotti, Senescence stimulates U937-endothelial cell interactions, Exp. Cell Res. 208 (1) (1993) 270–274.

[32] B. Hampel, K. Fortschegger, S. Ressler, M.W. Chang, H. Unterluggauer, A. Breitwieser, W. Sommergruber, B. Fitzky, G. Lepperdinger, P. Jansen-Durr, R. Voglauer, J. Grillari, Increased expression of extracellular proteins as a hallmark of human endothelial cell in vitro senescence, Exp. Gerontol. 41 (5) (2006) 474–481.

[33] J.P. Coppe, P.Y. Desprez, A. Krtolica, J. Campisi, The senescence-associated secretory phenotype: the dark side of tumor suppression, Annu. Rev. Pathol. 5 (2010) 99–118.

[34] Z. Wu, Y. Yu, C. Liu, Y. Xiong, J.P. Montani, Z. Yang, X.F. Ming, Role of p38 mitogen activated protein kinase in vascular endothelial aging: interaction with Arginase-II and S6K1 signaling pathway, Aging (Albany NY) 7 (1) (2015) 70–81.

[35] P. Davalli, T. Mitic, A. Caporali, A. Lauriola, D. D'Arca, ROS, Cell senescence, and novel molecular mechanisms in aging and age-related diseases, Oxid. Med. Cell. Longev. (2016) (2016) 3565127.

[36] H. Matsumoto, K. Ishikawa, H. Itabe, Y. Maruyama, Carbon monoxide and bilirubin from heme oxygenase-1 suppresses reactive oxygen species generation and plasminogen activator inhibitor-1 induction, Mol. Cell. Biochem. 291 (1–2) (2006) 21–28.

[37] T. Hayakawa, M. Iwai, S. Aoki, K. Takimoto, M. Maruyama, W. Maruyama, N. Motoyama, SIRT1 suppresses the senescence-associated secretory phenotype through epigenetic gene regulation, PLoS One 10 (1) (2015) e0116480.

[38] T. Liu, X. Ma, T. Ouyang, H. Chen, J. Lin, J. Liu, Y. Xiao, J. Yu, Y. Huang, SIRT1 reverses senescence via enhancing autophagy and attenuates oxidative stress-induced apoptosis through promoting p53 degradation, Int. J. Biol. Macromol. 117 (2018) 225–234.

[39] C. Sidrauski, A.M. McGeachy, N.T. Ingolia, P. Walter, The small molecule ISRIB reverses the effects of eIF2alpha phosphorylation on translation and stress granule assembly, Elife 4 (2015).

[40] M. Jedrusik-Bode, M. Studencka, C. Smolka, T. Baumann, H. Schmidt, J. Kampf, F. Paap, S. Martin, J. Tazi, K.M. Muller, M. Kruger, T. Braun, E. Bober, The sirtuin SIRT6 regulates stress granule formation in C. elegans and mammals, J. Cell Sci.126 (Pt 22) (2013) 5166–5177.

[41] G. Li Volti, D. Sacerdoti, B. Sangras, A. Vanella, A. Mezentsev, G. Scapagnini, J.R. Falck, N.G. Abraham, Carbon monoxide signaling in promoting angiogenesis in human microvessel endothelial cells, Antioxidants Redox Signal. 7 (5–6) (2005) 704–710.

[42] H. Segersvard, P. Lakkisto, M. Hanninen, H. Forsten, J. Siren, K. Immonen, R. Kosonen, M. Sarparanta, M. Laine, I. Tikkanen, Carbon monoxide releasing molecule improves

structural and functional cardiac recovery after myocardial injury, Eur. J. Pharmacol. 818 (2018) 57–66.

[43] J. Liu, A.L. Fedinec, C.W. Leffler, H. Parfenova, Enteral supplements of a carbon monoxide donor CORM-A1 protect against cerebrovascular dysfunction caused by neonatal seizures, J. Cereb. Blood Flow Metab. 35 (2) (2015) 193–199.

[44] H. Fujimoto, M. Ohno, S. Ayabe, H. Kobayashi, N. Ishizaka, H. Kimura, K. Yoshida, R. Nagai, Carbon monoxide protects against cardiac ischemia–reperfusion injury in vivo via MAPK and Akt–eNOS pathways, Arterioscler. Thromb. Vasc. Biol. 24 (10) (2004) 1848–1853.

[45] C. Focaccetti, A. Bruno, E. Magnani, D. Bartolini, E. Principi, K. Dallaglio, E.O. Bucci, G. Finzi, F. Sessa, D.M. Noonan, A. Albini, Effects of 5-fluorouracil on morphology, cell cycle, proliferation, apoptosis, autophagy and ROS production in endothelial cells and cardiomyocytes, PLoS One 10 (2) (2015) e0115686.

[46] J.P. Coppe, K. Kauser, J. Campisi, C.M. Beausejour, Secretion of vascular endothelial growth factor by primary human fibroblasts at senescence, J. Biol. Chem. 281 (40) (2006) 29568–29574.

[47] C. Lopez-Otin, M.A. Blasco, L. Partridge, M. Serrano, G. Kroemer, The hallmarks of aging, Cell 153 (6) (2013) 1194–1217.

[48] X. Chen, B.T. Andresen, M. Hill, J. Zhang, F. Booth, C. Zhang, Role of reactive oxygen species in tumor necrosis factor-alpha induced endothelial dysfunction, Curr. Hypertens. Rev. 4 (4) (2008) 245–255.

[49] C. Roma-Mateo, M. Seco-Cervera, J.S. Ibanez-Cabellos, E. Berenguer-Pascual, G. Perez, L.R. Rodriguez, J.L. Garcia-Gimenez, Oxidative stress and the epigenetics of cell senescence: insights from progeroid syndromes, Curr. Pharmaceut. Des. 24 (40) (2019) 4755–4770.

[50] A. Loboda, M. Damulewicz, E. Pyza, A. Jozkowicz, J. Dulak, Role of Nrf2/HO-1 system in development, oxidative stress response and diseases: an evolutionarily conserved mechanism, Cell. Mol. Life Sci. 73 (17) (2016) 3221–3247.

[51] H. Luo, L. Wang, B.A. Schulte, A. Yang, S. Tang, G.Y. Wang, Resveratrol enhances ionizing radiation-induced premature senescence in lung cancer cells, Int. J. Oncol. 43 (6) (2013) 1999–2006.

[52] T. Hayashi, H. Matsui-Hirai, A. Miyazaki-Akita, A. Fukatsu, J. Funami, Q.F. Ding, S. Kamalanathan, Y. Hattori, L.J. Ignarro, A. Iguchi, Endothelial cellular senescence is inhibited by nitric oxide: implications in atherosclerosis associated with menopause and diabetes, Proc. Natl. Acad. Sci. U. S. A. 103 (45) (2006) 17018–17023.

[53] M. Vasa, K. Breitschopf, A.M. Zeiher, S. Dimmeler, Nitric oxide activates telomerase and delays endothelial cell senescence, Circ. Res. 87 (7) (2000) 540–542.

[54] P.M. Yang, Y.T. Huang, Y.Q. Zhang, C.W. Hsieh, B.S. Wung, Carbon monoxide releasing molecule induces endothelial nitric oxide synthase activation through a calcium and phosphatidylinositol 3-kinase/Akt mechanism, Vasc. Pharmacol. 87 (2016) 209–218.

[55] I. Mattagajasingh, C.S. Kim, A. Naqvi, T. Yamamori, T.A. Hoffman, S.B. Jung, J. DeRicco, K. Kasuno, K. Irani, SIRT1 promotes endothelium-dependent vascular relaxation by

activating endothelial nitric oxide synthase, Proc. Natl. Acad. Sci. U. S. A. 104 (37) (2007) 14855–14860.

[56] H. Ota, M. Eto, S. Ogawa, K. Iijima, M. Akishita, Y. Ouchi, SIRT1/eNOS axis as a potential target against vascular senescence, dysfunction and atherosclerosis, J. Atheroscler. Thromb. 17 (5) (2010) 431–435.

[57] P. Anderson, N. Kedersha, RNA granules: post-transcriptional and epigenetic modulators of gene expression, Nat. Rev. Mol. Cell Biol. 10 (6) (2009) 430–436.

[58] K. Arimoto, H. Fukuda, S. Imajoh-Ohmi, H. Saito, M. Takekawa, Formation of stress granules inhibits apoptosis by suppressing stress-responsive MAPK pathways, Nat. Cell Biol. 10 (11) (2008) 1324–1332.

[59] A. Omer, D. Patel, X.J. Lian, J. Sadek, S. Di Marco, A. Pause, M. Gorospe, I.E. Gallouzi, Stress granules counteract senescence by sequestration of PAI-1, EMBO Rep. 19 (5) (2018).

[60] Martin TR, Wurfel MM. A TRIFfic perspective on acute lung injury. Cell. 2008 Apr 18;133(2):208-10.

[61] Ying Y, Mao Y, Yao M. NLRP3 Inflammasome Activation by MicroRNA-495 Promoter Methylation May Contribute to the Progression of Acute Lung Injury. Mol Ther Nucleic Acids. 2019 Dec 6; 18:801-814.

[62] Kong L, Deng J, Zhou X, Cai B, Zhang B, Chen X, Chen Z, Wang W. Sitagliptin activates the p62-Keap1-Nrf2 signalling pathway to alleviate oxidative stress and excessive autophagy in severe acute pancreatitis-related acute lung injury. Cell Death Dis. 2021 Oct 11;12(10):928.

[63] Li X, Shan C, Wu Z, Yu H, Yang A, Tan B. Emodin alleviated pulmonary inflammation in rats with LPS-induced acute lung injury through inhibiting the mTOR/HIF-1α/VEGF signaling pathway. Inflamm Res. 2020 Apr;69(4):365-373.

[64] Xie W, Lu Q, Wang K, Lu J, Gu X, Zhu D, Liu F, Guo Z. miR-34b-5p inhibition attenuates lung inflammation and apoptosis in an LPS-induced acute lung injury mouse model by targeting progranulin. J Cell Physiol. 2018 Sep;233(9):6615-6631.

[65] Qiang Z, Dong H, Xia Y, Chai D, Hu R, Jiang H. Nrf2 and STAT3 Alleviates Ferroptosis-Mediated IIR-ALI by Regulating SLC7A11. Oxid Med Cell Longev. 2020 Sep 18;2020:5146982.

[66] Cell Death Dis. 2021 Oct 29;12(11):1027.

[67] Stockwell BR, Friedmann Angeli JP, Bayir H, Bush AI, Conrad M, Dixon SJ, Fulda S, Gascón S, Hatzios SK, Kagan VE, Noel K, Jiang X, Linkermann A, Murphy ME, Overholtzer M, Oyagi A, Pagnussat GC, Park J, Ran Q, Rosenfeld CS, Salnikow K, Tang D, Torti FM, Torti SV, Toyokuni S, Woerpel KA, Zhang DD. Ferroptosis: A Regulated Cell Death Nexus Linking Metabolism, Redox Biology, and Disease. Cell. 2017 Oct 5;171(2):273-285.

[68] Dixon SJ, Lemberg KM, Lamprecht MR, Skouta R, Zaitsev EM, Gleason CE, Patel DN, Bauer AJ, Cantley AM, Yang WS, Morrison B 3rd, Stockwell BR. Ferroptosis: an iron-dependent form of nonapoptotic cell death. Cell. 2012 May 25;149(5):1060-72.

[69] Horsefield S, Burdett H, Zhang X, Manik MK, Shi Y, Chen J, Qi T, Gilley J, Lai JS, Rank MX, Casey LW, Gu W, Ericsson DJ, Foley G, Hughes RO, Bosanac T, von Itzstein M, Rathjen JP, Nanson JD, Boden M, Dry IB, Williams SJ, Staskawicz BJ, Coleman MP, Ve T, Dodds PN,

Kobe B. NAD^+ cleavage activity by animal and plant TIR domains in cell death pathways. Science. 2019 Aug 23;365(6455):793-799.

[70] Carty M, Kearney J, Shanahan KA, Hams E, Sugisawa R, Connolly D, Doran CG, Muñoz-Wolf N, Gürtler C, Fitzgerald KA, Lavelle EC, Fallon PG, Bowie AG. Cell Survival and Cytokine Release after Inflammasome Activation Is Regulated by the Toll-IL-1R Protein SARM. Immunity. 2019 Jun 18;50(6):1412-1424.

[71] Joe Y, Kim SK, Chen Y, Yang JW, Lee JH, Cho GJ, Park JW, Chung HT. Tristetraprolin mediates anti-inflammatory effects of carbon monoxide on lipopolysaccharide-induced acute lung injury. Am J Pathol. 2015 Nov;185(11):2867-74.

[72] Bayeva M, Khechaduri A, Puig S, Chang HC, Patial S, Blackshear PJ, Ardehali H. mTOR regulates cellular iron homeostasis through tristetraprolin. Cell Metab. 2012 Nov 7;16(5):645-57.

[73] Joe Y, Chen Y, Park J, Kim HJ, Rah SY, Ryu J, Cho GJ, Choi HS, Ryter SW, Park JW, Kim UH, Chung HT. Cross-talk between CD38 and TTP Is Essential for Resolution of Inflammation during Microbial Sepsis. Cell Rep. 2020 Jan 28;30(4):1063-1076.

[74] Liu X, Wang L, Xing Q, Li K, Si J, Ma X, Mao L. Sevoflurane inhibits ferroptosis: A new mechanism to explain its protective role against lipopolysaccharide-induced acute lung injury. Life Sci. 2021 Jun 15;275:119391.

[75] Conrad M, Kagan VE, Bayir H, Pagnussat GC, Head B, Traber MG, Stockwell BR. Regulation of lipid peroxidation and ferroptosis in diverse species. Genes Dev. 2018 May 1;32(9-10):602-619.

[76] Mukherjee P, Woods TA, Moore RA, Peterson KE. Activation of the innate signaling molecule MAVS by bunyavirus infection upregulates the adaptor protein SARM1, leading to neuronal death. Immunity. 2013 Apr 18;38(4):705-16.

[77] Zhao ZY, Xie XJ, Li WH, Liu J, Chen Z, Zhang B, Li T, Li SL, Lu JG, Zhang L, Zhang LH, Xu Z, Lee HC, Zhao YJ. A Cell-Permeant Mimetic of NMN Activates SARM1 to Produce Cyclic ADP-Ribose and Induce Non-apoptotic Cell Death. iScience. 2019 May 31; 15:452-466.

[78] Zhang Z, Guo M, Li Y, Shen M, Kong D, Shao J, Ding H, Tan S, Chen A, Zhang F, Zheng S. RNA-binding protein ZFP36/TTP protects against ferroptosis by regulating autophagy signaling pathway in hepatic stellate cells. Autophagy. 2020 Aug;16(8):1482-1505.

[79] Xue C, Wang Y, Guo Z, Wu Y, Zhen X, Chen M, Chen J, Xue S, Peng Z, Lu Q, Tai R. High-performance soft x-ray spectromicroscopy beamline at SSRF. Rev Sci Instrum. 2010 Oct;81(10):103502.

[80] Amadio P, Tarantino E, Sandrini L, Tremoli E, Barbieri SS. ProstaglandinEndoperoxide Synthase-2 deletion affects the natural trafficking of annexin A2 in monocytes and favours venous thrombosis in mice. Thromb Haemost. 2017;117(8):1486–97

[81] Hua X, Chi W, Su L, Li J, Zhang Z, Yuan X. ROS-induced oxidative injury involved in pathogenesis of fungal keratitis via p38 MAPK activation. Sci Rep. 2017;7(1):10421.

[82] Tang D, Chen X, Kang R, Kroemer G. Ferroptosis: molecular mechanisms and health implications. Cell Res. 2021 Feb;31(2):107-125.

[83] Su LJ, Zhang JH, Gomez H, Murugan R, Hong X, Xu D, Jiang F, Peng ZY. Reactive Oxygen Species-Induced Lipid Peroxidation in Apoptosis, Autophagy, and Ferroptosis. Oxid Med Cell Longev. 2019 Oct 13; 2019:5080843.

[84] Yang WS, SriRamaratnam R, Welsch ME, Shimada K, Skouta R, Viswanathan VS, Cheah JH, Clemons PA, Shamji AF, Clish CB, Brown LM, Girotti AW, Cornish VW, Schreiber SL, Stockwell BR. Regulation of ferroptotic cancer cell death by GPX4. Cell. 2014 Jan 16;156(1-2):317-331.

[85] Yang WS, Kim KJ, Gaschler MM, Patel M, Shchepinov MS, Stockwell BR. Peroxidation of polyunsaturated fatty acids by lipoxygenases drives ferroptosis. Proc Natl Acad Sci U S A. 2016 Aug 23;113(34): E4966-75.

[86] Carty M, Bowie AG. SARM: From immune regulator to cell executioner. Biochem Pharmacol. 2019 Mar; 161:52-62.